Coastal reservoirs as a source of nitrous oxide: spatio-temporal patterns and assessment strategy

Ping Yang[a,b], Miaohui Lu[a,b], Kam W. Tang[c], Hong Yang[d,e,f], Derrick Y. F. Lai[g], Chuan Tong[a,b*], Kwok Pan Chun[h], Linhai Zhang[a,b], Chen Tang[b]

[a]*Key Laboratory of Humid Subtropical Eco-geographical Process of Ministry of Education, Fujian Normal University, Fuzhou 350007, P.R. China*

[b]*School of Geographical Sciences, Fujian Normal University, Fuzhou 350007, P.R. China*

[c]*Department of Biosciences, Swansea University, Swansea SA2 8PP, U. K.*

[d]*College of Environmental Science and Engineering, Fujian Normal University, Fuzhou 350007, P.R. China*

[e]*Collaborative Innovation Center of Atmospheric Environment and Equipment Technology, Jiangsu Key Laboratory of Atmospheric Environment Monitoring and Pollution Control (AEMPC), School of Environmental Science and Engineering, Nanjing University of Information Science & Technology, 219 Ningliu Road, Nanjing 10044, China*

[f]*Department of Geography and Environmental Science, University of Reading, Reading, RG6 6AB, UK*

[g]*Department of Geography and Resource Management, The Chinese University of Hong Kong, Hong Kong, China*

[h]*Department of Geography, Hong Kong Baptist University, Hong Kong, China*

***Correspondence to:**

tongch@fjnu.edu.cn (Chuan Tong)

A B S T R A C T

Coastal reservoirs are widely regarded as a viable solution to the water scarcity problem faced by coastal cities with growing populations. As a result of the accumulation of anthropogenic wastes and the alteration of hydroecological processes, these reservoirs may also become the emission hotspots of nitrous oxide (N_2O). Hitherto, accurate global assessment of N_2O emission suffers from the scarcity and low spatio-temporal resolution of field data, especially from small coastal reservoirs with high spatial heterogeneity and multiple water sources. In this study, we measured the surface water N_2O concentrations and emissions at a high spatial resolution across three seasons in a subtropical coastal reservoir in southeastern China, which was hydrochemically highly heterogeneous because of the combined influence of river runoff, aquacultural discharge, industrial discharge and municipal sewage. Both N_2O concentration and emission exhibited strong spatio-temporal variations, which were correlated with nitrogen loading from the river and wastewater discharge. The mean N_2O concentration and mission were found to be significantly higher in the summer than in spring and autumn. The results of redundancy analysis showed that NH_4^+-N explained the greatest variance in N_2O emission, which implied that nitrification was the main microbial pathway for N_2O production in spite of the potentially increasing importance of denitrification of NO_3^--N in the summer. The mean N_2O emission across the whole reservoir was 107 $\mu g\ m^{-2}\ h^{-1}$, which was more than an order of magnitude higher than that from global lakes and reservoirs. Based on our results of

Monte Carlo simulations, a minimum of 15 sampling points per km^2 would be needed to produce representative and reliable N_2O estimates in such a spatially heterogeneous aquatic system. Overall, coastal reservoirs could play an increasingly important role in future climate change via their N_2O emission to the atmosphere as water demand and anthropogenic pressure continue to rise.

Keywords: Greenhouse gases; Water management; itrous oxide; Spatial heterogeneity; Wastewater discharge; Coastal reservoir

1. Introduction

Over 30 % of the world's population currently live in water-scarce regions (United Nations, 2018). In many of these regions, water scarcity is caused not by water shortage but rather insufficient water storage, leading to the construction of reservoirs as one of the common solutions to help divert and retain surface runoff (Sitharam et al., 2020). Coastal reservoirs are particularly appealing because of their low cost, low ecological impacts on upstream areas, and close proximity to the coastal populations with growing water demand (Liu et al., 2013). Coastal reservoirs are considered a key water management solution in densely populated coastal cities around the world by providing portable water for irrigation, preventing flooding downstream, and treating the discharged wastewater (Sitharam et al., 2020).

By retaining surface runoff and lengthening the water residence time, coastal reservoirs may accumulate pollutants and alter various hydroecological processes, leading to the release of greenhouse gases (e.g., nitrous oxide or N_2O) into the atmosphere. This is of particular concern for reservoirs in densely populated areas with high loadings of nutrients and wastes. In general, high nutrient loadings will increase the microbial-mediated process of N_2O production (Davidson et al., 2015; Wang et al., 2017; Xiao et al., 2019a), subsequently triggering more N_2O emission from reservoirs to the atmosphere (Wang et al., 2017; He et al., 2017). In addition, high nutrient loads in the reservoirs can drive large oxygen depletion, further promoting denitrification as the primary pathway of N_2O production (Borges et al., 2015). Dammed rivers and

reservoirs are thus potentially N_2O emission hotspots.

N_2O is a highly potent greenhouse gas with a global warming potential almost 300 times higher than that of carbon dioxide (CO_2) over a 100-year period (IPCC, 2013), and is also one of the major ozone-depleting substances (Ravishankara et al., 2009; Shaaban et al., 2018). The average atmospheric N_2O concentration reached 331 ppbv in 2018, which was approximately 23% above the pre-industrial level (World Meteorological Organization, 2019) with a growth rate of 0.7–0.8 ppb yr^{-1} over the last three decades (Davidson, 2009; Saikawa et al., 2014; Xiao, et al., 2019a). Despite the climatic importance of N_2O, accurate assessment of N_2O emissions are limited by the low availability of field data and the use of emission factor (EF) that is associated with the background N stock only. While it may be appropriate to apply EF for agriculture-based emission with easily quantifiable N input from fertilizers, applying specific EF in aquatic systems may yield large errors in the estimation of N_2O emission (Maavara et al., 2019), because of the highly variable N dynamics in both quantity and quality (Ivens et al., 2011). Furthermore, the assessment of N_2O emission is often done at low spatial resolutions (e.g., 1°×1° grids), which is too crude for small coastal reservoirs with high hydrographical heterogeneity and multiple water sources.

To address these limitations and explore the potential importance of coastal reservoirs as a net N_2O source, we measured in this study the surface water N_2O concentrations at a high spatial resolution in a subtropical coastal reservoir in southeast China, from which we calculated N_2O emissions using the wind-based thin boundary

layer model. We also examined the influence of environmental factors on the spatial variations of N_2O emissions and determined the optimal sampling strategy for assess N_2O emissions from spatially heterogeneous water bodies.

2. Materials and methods

2.1. Study area

The Wenwusha Reservoir (25°49′36″–25°54′00″ N, 119°35′12″–119°38′11″ E) is a coastal reservoir located at the mouth of the Nangyangdong River in Fujian Province in southeast China (Fig. 1). It has a surface area of 5.2 km^2, a mean depth of 9.0 m, a total volume of 3.20×10^8 m^3 and a catchment area of 275 km^2 (Yang et al., 2020a). Influenced by a humid subtropical monsoonal climate, this reservoir has an annual mean temperature of 19.3 °C and an annual precipitation of 1390 mm, with 75% of the precipitation occurring during the wet season (May - September).

The reservoir is divided into two basins, namely the north basin (NB) and the south basin (SB) (Fig. 1) (Yang et al., 2020a). NB (1.9 km^2; 1.40×10^8 m^3) is located in an urbanized area and is heavily impacted by aquacultural, industrial and municipal waste discharges while also receiving input from the Nanyangdong River. On the other hand, the watershed of SB (3.3 km^2; 1.69×10^8 m^3) is dominated by natural wetlands and forests. This study covered a total of 10 transects in NB and 11 transects in SB, with 3-10 sampling sites selected along each transect (Fig. 1). A total of 103 sampling

sites (56 in NB and 47 in SB) were included, which could be categorized into five different sections according to the types of discharge: industrial effluents (Section-I; n = 4), town sewage (Section-T; n = 6), river inputs (Section-R; n = 7), aquacultural waste (Section-A; n = 22) and non-wastewater discharge (Section-N; n = 64).

2.2. Dissolved N_2O concentrations

Three sampling surveys covering the entire reservoi were conducted in November 2018, March 2019, and June 2019, respectively. In each survey, sample collection was completed within two consecutive days. We collected water samples at 20 cm depth using a 100-mL syringe equipped with three-way stopcock, and quickly transferred them into 55-mL glass serum bottles. We added 0.2 mL of saturated $HgCl_2$ into each bottle to inhibit microbial activities (Taipale and Sonninen 2009; Zhang et al., 2013), and then immediately sealed the bottle with an open-topped screw cap equipped with a halobutyl rubber septum to exclude air bubbles (Borges et al., 2018; Xiao et al., 2019a; Yang et al., 2020b). All the water samples were stored in an ice box and analyzed within 48 hours of collection.

Dissolved N_2O concentrations were measured following the headspace equilibration method (Yu et al., 2013; Yu et al., 2017). In the laboratory, N_2 gas (>99.9% purity) was injected into each sample bottle to displace a 25-mL headspace. The bottles were then shaken vigorously for 10 minutes in an oscillator to gas achieve an

equilibrium in N_2O between the headspace air and the liquid phase. After waiting for 30 minutes, 5 mL of headspace air sample was collected with a syringe and analyzed for N_2O concentration using a gas chromatograph (GC-2014, Shimadzu, Kyoto, Japan) equipped with an electron capture detector. The detection limit was 0.02 ppm and the relative standard deviations of the measurements were ≤ 5.0% (Yang et al., 2020b). Dissolved N_2O concentration was then calculated based on the temperature, Henry's law constant (salinity-dependent) and the measured head space N_2O concentration according to Weiss and Price (1980).

2.3. N_2O emission

N_2O emission ($F_{W\text{-}A}$, μmol m^{-2} h^{-1} was calculated using the thin boundary layer model (Equation 1) that has been widely applied in the lentic ecosystem (e.g., Cole and Caraco, 1998; Musenze et al., 2014 Xiao et al., 2019b):

$$F_{W\text{-}A} = k \times (C_{obs} - C_{eq}) \quad \text{(Eq1)}$$

where k is the gas transfer velocity (m h^{-1}); C_{obs} is the measured N_2O concentration (nmol L^{-1}) in the surface water; C_{eq} is the dissolved N_2O concentration (nmol L^{-1}) in equilibrium with the atmospheric concentration at the prevailing *in situ* conditions, as a function of atmospheric pressure, water temperature, and the ambient atmospheric N_2O.

Because of negligible surface water flow at the reservoir, the N_2O transfer velocity is primarily controlled by wind speed (Xiao et al., 2019b). In this study, we calculated k value using a wind-dependent equation (Eq 2) for small shallow lakes (Cole and Caraco,

1998):

$$k = (Sc/660)^{-n}(2.07 + 0.215 \times U_{10}^{1.7}) \quad \text{(Eq 2)}$$

where Sc is the temperature-dependent Schmidt number for N_2O; n is a constant that varies between 0.66 (for wind speeds ≤3 m s^{-1}) and 0.50 (wind speeds >3 m s^{-1}); U_{10} is the frictionless wind speed (m s^{-1}) at 10 m height. Sc and U_{10} were calculated using the following equations (Crusius and Wanninkhof, 2003; Wanninkhof, 1992):

$$Sc = 2055.6 - 137.11T + 4.3173T^2 - 0.054350\,T^3 \quad \text{(Eq 3)}$$

$$U_{10} = U_z[1 + \frac{(C_{d10})^{1/2}}{K} \ln(\frac{10}{z})] \quad \text{(Eq 4)}$$

where U_z is the wind speed (m s^{-1}) at a ght of z above the water surface (2.0 m in this study); C_{d10} is the drag coefficient at 10 m above the water surface (0.0013 m s^{-1}); and K is the von Karman constant (0.41).

2.4. Environmental variables

Water samples were collected at a depth of 20 cm with a 5 L organic glass hydrophore and transferred into 150 mL polyethylene bottles. About 0.5 mL of saturated $HgCl_2$ solution was added to inhibit microbial activities (Zhang et al., 2013). The water samples were transported in an ice box back to the laboratory for analysis. In the laboratory, the water sample was filtered through a 0.45-μm cellulose acetate filter (Biotrans™) and then analyzed for the concentrations of total dissolved nitrogen (TDN), ammonium-nitrogen (NH_4^+-N), and nitrate-nitrogen (NO_3^--N) using a flow injection

analyzer (Skalar Analytical SAN^{++}, The Netherlands) (Yang et al., 2020b). The detection limit and relative standard deviations were 3.0 μg L^{-1} and ≤2.0% for TDN, 0.6 μg L^{-1} and ≤3.0% for NH_4^+-N and 0.6 μg L^{-1} and ≤2.0% for NO_3^--N.

Concurrent measurements of water temperature (T_W) and pH (IQ150 pH/mV/Temperature meter, IQ Scientific Instruments, USA), salinity (Eutech Instruments-Salt6 salinity meter, USA), dissolved oxygen (DO; 550A YSI sonde, USA) and electrical conductivity (EC; 2265FS electrical conductivity meter, Spectrum Technologies, USA) were also made at a water depth of 20 cm (Yang et al., 2020a). The relative standard deviations of the measurements were between ≤1.0% and ≤2.0%. Air temperature (T_A), wind speed at 2 m height (W_S) and atmospheric pressure (P_{atm}) were measured by a portable weather meter (Kestrel-3500, USA).

2.5. Statistical analysis

Results were presented as mean ± 1 standard error. Significant differences in hydrographical properties, dissolved N_2O concentration and N_2O emission among reservoir basins and discharge sections were tested by analysis of variance (ANOVA) using the statistical software SPSS 17.0 (SPSS Inc., USA). Correlations between hydrographical parameters and N_2O concentration or emissions were investigated by Pearson correlation analysis. The extent to which environmental variables affected the spatiotemporal variations in N_2O emissions was tested by Redundancy Analysis (RDA) using the software CANOCO 5.0 (Microcomputer Power, Ithaca, USA), with T_W, pH,

DO, salinity, NO_3^--N and NH_4^+-N, and TDN being inputted as environmental variables.

Monte Carlo analysis was used to determine the optimal sample size for assessing the mean N_2O emission at the whole-reservoir scale. The measured fluxes were resampled from the 103 sites with varying sample sizes (n = 10, 20, 30…, 100) without replacement for 10,000 times. The overall mean and standard deviation of N_2O emission were subsequently calculated for each sample size. Plots were created using OriginPro 7.5 (OriginLab Corp. USA). To illustrate the spatial variations in hydrographical parameters and N_2O concentration (or flux) in the reservoir, the Kriging method in ArcGIS 10.2 (ESRI Inc., Redlands, CA, USA) was employed for spatial interpolation.

3. Results

3.1. Hydrographical parameters

There were large differences in hydrographical parameters between NB and SB across the three campaigns. NB had lower DO, EC, and salinity (Fig. S1) and higher NO_3^--N, NH_4^+-N and TDN concentrations as compared to SB (Fig. 2). T_W and pH were comparable between the two basins (Fig. S2). Water chemistry also varied spatially depending on the discharge types. In Section-N without sewage discharge, the NO_3^--N, NH_4^+-N, and TDN concentrations were significantly lower (p<0.05) while DO and salinity were generally higher than in other sections.

The hydrographical parameters also showed strong temporal variation across the whole reservoir (p<0.001). Average water temperature was 23.6 ºC during the study period, while the seasonal pattern was clear decreasing in the order: summer (29.3 ºC) > spring (23.1 ºC) > autumn (18.3 ºC) (Fig. S2). The seasonal mean concentrations of NO_3^--N, NH_4^+-N and TDN ranged from 0.95 to 1.47, 0.28 to 0.57, and 1.43 to 1.82 mg L^{-1}, respectively. The seasonal mean DO concentration, pH and salinity ranged from 4.60 to 8.87 mg L^{-1}, 6.88 to 10.70, and 0.41 to 1.49‰, respectively. We observed generally higher NO_3^--N, TDN, pH and salinity in autumn (Fig. 2 and Fig. S1), but higher DO and lower NH_4^+-N in spring (Fig. 2 and Fig. S1). The seasonal mean water depth ranged from 6.0 to 8.6 m, with a maximum value occurring in summer.

3.2. Spatial variation in N_2O concentration

Surface water N_2O concentrati in the reservoir showed high spatial heterogeneity, varying by 9 to >30 folds between the two basins (Fig. 3a-3c). The mean N_2O concentrations were significantly higher in NB than in SB (Table 1), while the overall mean N_2O concentrations in November, March and June were 46.4±2.0, 58.9±5.9, and 43.9±2.7 nmol L^{-1}, respectively.

N_2O concentration also varied spatially depending on the discharge types, with significantly lower values in Section-N (non-wastewater discharge) and generally higher values in Section-T (town sewage) (Table 1). Overall, N_2O concentration showed significant differences between the sections with and without wastewater

discharge (Fig. 4a-4c).

3.3. Spatial variation in N_2O emission

From November to June, N_2O emission varied spatially by from >100 to >300 folds between the two basins (Fig. 3d-3f). N_2O emissions were generally high in NB, ranging from 6.9 to 711.5 μg m^{-2} h^{-1} with a mean of 153.1±8.6 μg m^{-2} h^{-1}. In contrast, N_2O emissions were significantly lower in SB (Table 1), with occasional occurrence of negative values (i.e. net uptake of N_2O). The reservoir-wide mean N_2O emissions were 110.4±9.3, 78.5±6.3, and 153.1±8.6 μg m^{-2} h^{-1} in November, March, and June, respectively.

There were clear spatial differences in N_2O emission as a function of discharge types, with lower emissions in Section-N without wastewater discharge but higher emissions in Section-I (industrial effluent) and Section-R (river runoff) across the three seasons (Table 1). Overall, there were significant differences in mean N_2O emission between the sections with and without wastewater discharge (Fig. 4d-4f).

3.4. Effects of environmental variables on N_2O concentration and emission

Results of Pearson correlation analysis showed that the reservoir-wide N_2O concentration and emission were correlated negatively with DO, EC, and salinity (Table S2) and correlated positively with NO_3^--N, NH_4^+-N and TDN concentrations across all surveys (Table S2, Fig. S3 and S4). Over the whole study period, the N_2O concentration and flux in the reservoir were positively correlated with air temperature but negatively

correlated with wind speed (p<0.05 or < 0.01; Table S2). Atmospheric pressure had no significant correlation with either N_2O concentration or flux (p>0.05; Table S2).

Based on the result of RDA analysis, EC, TDN and NO_3^--N were the environmental variables that explained the most spatial variations in N_2O concentration and emission in November, March, and June, respectively (Fig. 5). Combining all the data together, NH_4^+-N had the largest explanatory power (50.4%) for the spatio-temporal variations in N_2O concentration and emission, followed by NO_3^--N (23.5%) and salinity (20.2%) (Fig. 5).

3.5. Determining the optimal sample size

Based on the results of Monte rlo analysis, the uncertainty of mean N_2O emission estimates across the reservoir decreased markedly with increasing number of sampling sites. For each sample size, we created the boxplots of N_2O resampling means after 10,000 times of resampling (Fig. 6a). The Highest Probability Density ranges converged with increasing sample size, indicating improved accuracy of N_2O emission. In addition, the bias of the resampling N_2O estimations declined and the standard deviations of resampling means decreased exponentially with sample size (Fig. 6b). Notably, an increase in sample size from 10 to 100 decreased the relative standard deviation of mean N_2O emission by nearly 20-fold, from 21% to 1.2%.

The results of Monte Carlo analysis could also be used to determine the optimal sample size for assessing the reservoir N_2O emission. To achieve an error of under 5%,

at least 80 samples over the whole reservoir (5.2 km^2) or ca. 15 samples per km^2 would be needed to resolve the high spatial heterogeneity of N_2O emissions. With a sample size of only 10, we obtained a high relative standard deviation of estimated average N_2O emission of 22.6% after 10,000 times of resampling. Despite this large deviation, the median of the resampled means was 107 μmol m^{-2} h^{-1} (Fig. 6a), which was close to the overall mean of all 103 samples combined. Therefore, the high spatial resolution measurements across multiple transects effectively reduced the estimation bias of N_2O emission in our study.

4. Discussion

4.1. N_2O production in reservoir systems

N_2O production is driven by microbial transformation of N substrates (Herrman et al., 2008; Liu et al., 2011; Phanwilai et al., 2020; Xiao et al., 2019b). Previous studies have reported significant relationships between sewage input, N substrates and N_2O emission in lakes (e.g., Xiao et al., 2019a), coastal river network (Yu et al., 2013) and inland reservoirs (e.g., He et al., 2017; Liu et al., 2011, 2017). In this study, while several environmental variables such as air temperature, wind speed, atmospheric pressure and solar radiation were quite homogeneous across the reservoir, the availability of N substrates as reflected by the concentrations of NH_4^+-N, NO_3^--N and TDN showed high spatial variations (Fig. 2). Both the concentrations of N substrate and

N_2O emission rates were much higher in the north basin than in the south basin (Table 1). Located in an urbanized region, our reservoir was heavily impacted by anthropogenic activities, particularly the discharge of domestic and industrial wastewaters and the nutrient-rich effluents from aquaculture ponds. The highest average NO_3^--N and NH_4^+-N concentrations were found in the section with river input, indicating the pronounced influence of the upstream area as a N source. In contrast, the N-section without wastewater discharge had better water quality as reflected by the lower NO_3^--N and NH_4^+-N concentrations and higher DO level (Table S1). Taken together, our results showed that the high spatial he erogeneity of N_2O emission was closely linked to the input of localized N subst ate into the reservoir.

N_2O can be produced via denitrification of NO_3^- under oxygen-poor conditions, or nitrification of NH_4^+-N under aer bic conditions. The DO levels obtained in this reservoir were generally high enough (ca. ≥ 25% sat.) to favor nitrification process (Fig. S1), which was further supported by the results of RDA analysis in which NH_4^+-N explained the largest overall variance in N_2O emission (ca. 50%) during the study period (Fig. 5d). However, it should be noted that DO was only measured in the surface water in this study, but could drop to lower levels in deeper water, especially during the summer, where denitrification might dominate. This hypothesis was supported by the results of RDA analysis in which NO_3^--N explained >73% of the variance in N_2O emission in June (Fig. 5c) when the average DO level was slightly lower (Table S1) and was the second most important factor in accounting for the overall variance (ca. 24%)

(Fig 5d). Interestingly, salinity also explained about 20% of the variance in N_2O emission (Fig. 5d). Because of the proximity of the south basin to the sea, salt intrusion and deposition has created spatial differences in salinity across the reservoir, which could adversely impact the abundance and activity of nitrifiers that are of freshwater in origin (Francis et al., 2003; Monteiro et al., 2017) and subsequently decrease N_2O production (Sun et al., 2013; Wang et al., 2018; Welti et al., 2017).

4.2. Spatial and temporal variations in N_2O emission

Large spatial variations in N_2O emission have been observed in freshwater lakes and reservoirs (Cheng et al., 2019; Musenze et al., 2014; Zhao et al., 2013). Based on field measurements with a high spatia resolution, we successfully characterized the spatial heterogeneity of N_2O emission from the Wenwusha Reservoir, which exhibited coefficients of variation ranging from 81% to 110% across the three seasons. Land use change in the catchment can disturb various biogeochemical processes on land and in adjacent waters (Hosen et al., 2014; Williams et al., 2016), with the consequence of changing the direction and magnitude of N_2O fluxes among different areas (He et al., 2017; Wang et al., 2017; Zhou et al., 2017). In our study, the concentrations of nitrogen substrate (NO_3^--N, NH_4^+-N, and TDN) were substantially lower in sites without wastewater discharge than in those in close proximity with aquaculture ponds, municipal and agricultural lands with wastewater discharge (Table S1). The N_2O concentration and flux increased with nitrogen concentration across the whole reservoir. Most notably, the sites under the influence of wastewater discharge covered only 30%

of the reservoir area but contributed to approximately 60% of the total N_2O emission from the whole reservoir. Our results demonstrated that the spatial variation in N_2O flux in the subtropical Wenwusha reservoirs was largely affected by various anthropogenic activities (e.g., urbanization and land use) in the catchment area.

N_2O emission also exhibited clear seasonal variation with significantly higher values in the summer (Table 1), similar to the observations made in other inland waters (Musenze et al., 2014; Xiao et al., 2019b; Zhu et al., 2013). Temperature is considered a dominant factor driving the temporal variation in N_2O emission by regulating microbial activity (Beaulieu et al. 2010; Harrison and Matson, 2003; Hinshaw and Dahlgren 2013). The higher N_2O emission observed in the summer coincided with the higher water temperature (Fig. S2c), which could have stimulated N_2O production. Interestingly, we observed that the verage N_2O emission in spring was substantially lower than that in autumn (Fig. 3 and Table 1), which were opposite to the trend with water temperature (Fig. S2a and S2b). There were several heavy rain events that occurred in spring. Previous studies have shown that heavy precipitation could transport a greater amount of nutrients and greenhouse gases from the surrounding watershed into the lentic ecosystems (Dinsmore et al., 2013; Sinha et al., 2017; Xiao et al., 2021), thereby increasing the saturation level of dissolved greenhouse gases and stimulating microbial greenhouse gas production (Stanley et al., 2016; Yu et al., 2017). However, we found no significant increase in dissolved N_2O concentrations and fluxes in association with the heavy spring precipitation, which was probably a result of the

dilution effects of precipitation on the biogeochemical reactions in the reservoir (Outram and Hiscock, 2012; He et al. 2017).

Furthermore, the drainage of aquaculture ponds after harvest in autumn as a common management practice could introduce N-rich effluent into the reservoir and stimulate N_2O production. This was supported by the elevated concentrations of NO_3^--N, NH_4^+-N, and TDN found near the aquaculture ponds in November (Fig. 2) and the strong positive correlations detected between N_2O emission and the concentration of N substrates (Fig. S4).

4.3. Subtropical coastal reservoir as a net N_2O source

The average N_2O fluxes across the water-air interface from the Wenwusha Reservoir was 107.0±15.6 μg m^{-2} h^{-1}, which was about 3.9 and 1.9 times higher than that observed in the marsh (Wang et al., 2018) and aquaculture ponds (Yang et al., 2020b), respectively, in the same subtropical coastal region. This magnitude of N_2O emission was also substantially higher than the average rate reported in the lakes (12.2 μg m^{-2} h^{-1}) and reservoirs (42.3 μg m^{-2} h^{-1}) of China (Li et al., 2018). When compared with the N_2O emission rates globally (Table S3), the mean emission from our reservoir was lower than only a handful of tropical or subtropical reservoirs, but was over an order of magnitude greater than the global average of 7.2 μg m^{-2} h^{-1} for lakes and reservoirs spanning across the tropical to polar regions (Hu et al., 2016). Our results, along with similar findings by others (Chen et al., 2014), suggested that subtropical

coastal reservoirs were strong N_2O sources and could play an increasingly important climatic role as countries seek to construct more coastal reservoirs (Yang and Kelly, 2015).

4.4. Implications for N_2O assessment and reservoir management

Over the past two decades, researchers have increasingly recognized the role of reservoirs as a potential source of greenhouse gases including N_2O (Deemer et al., 2016; Descloux et al., 2017; Maavara et al., 2019). However, reliable assessment of N_2O emission from global reservoirs remains a challenge due to the scarcity and low resolution of field data. Results from this study highlighted the high spatial and temporal heterogeneities of N_2O concentration and emission in a subtropical coastal reservoir, with significant implications to representative sampling for flux estimation. Our results of Monte Carlo analysis suggested that reliance of field data from only one or a few sampling points, as quite commonly done in the literature (Table S3), could yield large errors. Urbanized, coastal reservoirs such as the one studied here are often influenced by runoff and discharge from multiple sources. Our Monte Carlo simulation results (section 3.5) suggested that a minimum of 15 sampling points per km^2 would be needed to produce a reliable and representative estimate of spatially-averaged N_2O emission in the spatially heterogeneous coastal reservoir system.

Our data showed a strong correlation between N_2O emission and wastewater discharges, affirming the important role of wastewater input in promoting N_2O

emission. This problem of greenhouse gas release can be exacerbated by the race to modernization and urbanization, particularly in developing countries where wastewater treatment remains inadequate (Hosen et al., 2014; Williams et al., 2016; Yang et al., 2013). Strengthening environmental regulation, particularly for wastewater treatment and discharge, will be key to mitigate water pollution and greenhouse gas emission in reservoir management (Yang, 2014; Yang et al., 2015). To the best of our knowledge, this study was the first attempt to characterize N_2O concentration and emission from a coastal reservoir at a very high spatial resolution. Our data would be valuable for global biogeochemical modelling and prediction of N_2O emission from costal reservoirs that are under intense human disturbance.

Several aspects of our study could be improved further in future studies. Firstly, several studies in inland waters have reported diurnal variations with higher N_2O emissions at night (Baulch et al., 2012; Wu et al., 2018; Yang et al., 2011). Our measurements in the Wenwusha Reservoir were limited to daytime and therefore the emission might have been underestimated. Diurnal differences in N_2O emission from the reservoir should be compared to improve the reliability of flux estimates. Secondly, in a thermally stratified water column, nitrogen transformation can differ between the epilimnion and the hypolimnion (Beaulieu et al., 2015; Liang et al., 2019; Salk et al., 2016), which was not included in our study. Future studies might use novel methods such as isotopic tracing to examine the relative importance of different nitrogen biogeochemical processes throughout the water column (Sebilo et al., 2006). While we

aimed to resolve the spatial heterogeneity with high spatial resolution sampling, our data also showed considerable seasonal variations in N_2O concentration and emission (Fig. 4). However, resolving temporal variation at a higher frequency (monthly to daily) could be challenging logistically without the help of *in situ* automated sampling systems. Lastly, the microbial abundance and functional groups (e.g. nitrifier, denitrifier, and ammonifier) should be further characterized to shed light on the dominant microbial pathways of N_2O production in the reservoir.

5. Conclusions

We characterized the variation of N_2O concentration and emission in a coastal, urbanized reservoir in southeastern China with a high spatial resolution in this study. We found that N_2O concentration and emission were strongly influenced by localized runoff and discharges, resulting in very high spatial heterogeneity in addition to the seasonal variations. Results of Monte Carlo simulations showed that a minimum of 15 sampling points per km^2 would be required to produce a reliable estimate of the whole-reservoir N_2O emission. Based on the analysis of water chemistry data, nitrification appeared to be the main pathway for N_2O production, although denitrification might become increasingly important in the summer months with reducing DO level. Total N_2O emission from our subtropical coastal reservoir was estimated to be 4.8 Mg yr^{-1}, which was considerably higher than the global average for

lakes and reservoirs. Continued construction of coastal reservoirs for water management may exacerbate future climate change by increasing N_2O emission.

Declaration of competing interest

The authors declare that they have no known competing financial interests or personal relationships that could have appeared to influence the work reported in this paper.

Acknowledgements

This research was supported by the National Science Foundation of China (No. 41801070, 41671088), the National Science Foun ion of Fujian Province (No. 2018J01737), the Research Grants Council of the Hong Kong Special Administrative Region, China (CUHK458913), and the CUHK Direct Grant (SS15481), Open Research Fund Program of Jiangsu Key Laboratory of Atmospheric Environment Monitoring & Pollution Control (KHK1806), A projected funded by the Priority Academic Program Development of Jiangsu Higher Education Institutions (PAPD) and the Minjiang Scholar Programme. We would like to thank Yifei Zhang, Guanghui Zhao and Ling Li of the School of Geographical Sciences, Fujian Normal University, for their field assistance.

References

Baulch, H.M., Dillon, P.J., Maranger, R., Venkiteswaran, J.J., Wilson, H.F., Schiff, S.L., 2012. Night and day: short term variation in nitrogen chemistry and nitrous oxide emissions from streams. Freshwater Biol. 57, 509–525. https://doi.org/10.1111/j.1365-2427.2011.02720.x

Beaulieu, J.J., Nietch, C.T., Young, J.L., 2015. Controls on nitrous oxide production and consumption in reservoirs of the Ohio River Basin. J. Geophys. Res. Biogeosci. 120(10), 1995–2010. https://doi.org/10.1002/2015JG002941

Beaulieu, J.J., Tank, J.L., Hamilton, S.K., Wollheim, W.M., Hall Jr., R.O., Mulholland, P.J., Peterson, B.J., Ashkenas, L.R., Cooper, L.W., Dahm, C.N., Dodds, W.K., Grimm, N.B., Johnson, S.L., McDowell, W.H., Poole, G.C., Valett, H.M., Arango, C.P., Berno M.J., Burgin, A.J., Crenshaw, C.L., Helton, A.M., Johnson, L.T., O'Brien, J.M., Potter, J ., Sheibley, R.W., Sobota, D.J., Thomas, S.M., 2011. Nitrous oxide emission from de ification in stream and river networks. Proc. Natl. Acad. Sci. U.S.A. 108, 214−219. https://doi.org/10.1073/pnas.1011464108

Borges, A.V., Darchambeau, F., Teodoru, C.R., Marwick, T.R., Tamooh, F., Geeraert, N., Omengo, F.O., Gu´erin, F., Lambert, T., Morana Okuku, E., Bouillon, S., 2015. Globally significant greenhouse-gas emissions from African inland waters. Nat. Geosci. 8 (8), 637–642. https://doi.org/10.1038/NGEO2486

Borges, A.V., Speeckaert, G., Champenois, W., Scranton, M.I., Gypens, N., 2018. Productivity and temperature as drivers of seasonal and spatial variations of dissolved methane in the Southern Bight of North Sea. Ecosystems 21(4), 583−599. https://doi.org/10.1007/s10021-017-0171-7.

Chen, N.W., Chen, Z.H., Wu, Y.Q., Hu, A.Y., 2014. Understanding gaseous nitrogen removal through direct measurement of dissolved N_2 and N_2O in a subtropical river-reservoir system. Ecol. Eng. 70, 56–67. https://doi.org/10.1016/j.ecoleng.2014.04.017

Cheng, F., Zhang, H.M., Zhang, G.L., Liu, S.M., Song, G.D., Du, G.X., 2019. Distribution and emission of N_2O in the largest river-reservoir system along the Yellow River. Sci. Total Environ. 666, 1209–1219. https://doi.org/10.1016/j.scitotenv.2019.02.277

Cole, J.J., Caraco, N.F., 1998. Atmospheric exchange of carbon dioxide in a low-wind oligotrophic lake measured by the addition of SF_6. Limnol. Oceanogr. 43, 647−656. https://doi.org/10.4319/lo.1998.43.4.0647

Crusius, J., Wanninkhof, R., 2003. Gas transfer velocities measured at low wind speed over a lake. Limnol. Oceanogr. 48(3), 1010-1017.

Davidson, E.A., 2009. The contribution of manure and fertilizer nitrogen to atmospheric nitrous oxide since 1860. Nat. Geosci. 2, 659-662. https://doi.org/10.1038/ngeo608

Davidson, T.A., Audet, J., Svenning, J. ¯C., Lauridsen, T.L., Søn gaard, M., Landkildehus, F., Larsen, S.E., Jeppesen, E., 2015. Eutrophication effect n greenhouse gas fluxes from shallow-lake mesocosms override those of climate warming. Global Change Biol. 21, 4449−4463. https://doi.org/10.1111/gcb.13062

Deemer, B.R., Harrison, J.A., Li, S.Y., Beaulieu, J.J., Delsontro, T., Barros, N., Bezerra-Neto, J.F., Powers, S.M., Santos, M.A.D., Vonk, J.A., 2016. Greenhouse gas emissions from reservoir water surfaces: a new g l synthesis. BioScience 66, 949−964. https://doi.org/10.1093/biosci/biw117

Descloux, S., Chanudet, V., Serça, D., G rin, F., 2017. Methane and nitrous oxide annual emissions from an old eutrophic temperate reservoir. Sci. Total Environ. 598, 959−972. https://doi.org/10.1016/j.scitotenv.2017.04.066

Dinsmore, K.J., Billett, , Dyson, K.E., 2013. Temperature and precipitation drive temporal variability in aquatic arbon and GHG concentrations and fluxes in a peatland catchment. Glob. Chang. Biol. 19, 2133–2148. https://doi.org/10.1111/gcb.12209

Francis, C.A., O'Mullan, G.D., Ward, B.B., 2003. Diversity of ammonia monooxygenase (*amoA*) genes across environmental gradients in Chesapeake Bay sediments. Geobiology 1, 129−140. https://doi.org/10.1046/j.1472-4669.2003.00010.x

Harrison, J., Matson, P., 2003. Patterns and controls of nitrous oxide emissions from waters draining a subtropical agricultural valley. Glob. Biogeochem. Cy 17. https://doi.org/10.1029/2002GB001991

He, Y.X., Wang, X.F., Chen, H., Yuan, X.Z., Wu, N., Zhang, Y.W., Yue, J.S., Zhang, Q.Y., Diao, Y.B., Zhou, L.L., 2017. Effect of watershed urbanization on N_2O emissions from the Chongqing metropolitan river network, China. Atmos. Environ. 171, 70−81. https://doi.org/10.1016/j.atmosenv.2017.09.043

Herrman, K.S., Bouchard, V., Moore, R.H., 2008. Factors affecting denitrification in agricultural headwater streams in Northeast Ohio, USA. Hydrobiologia 598, 305−314. https://doi.org/10.1007/s10750-007-9164-4

Hinshaw, S. E., and R. A. Dahlgren. 2013. Dissolved nitrous oxide concentrations and fluxes from the eutrophic San Joaquin River, California. Environ. S Technol. 47, 1313−1322. https://doi.org/10.1021/es301373h

Hu, M., Chen, D., Dahlgren, R.A., 2016. Modeling nitr oxide emission from rivers: a global assessment. Glob. Chang. Biol. 22, 3566−3582. https://doi.org/10.1111/gcb.13351

Hosen, J.D., McDonough, O.T., Febria, C.M., Palmer, M.A., 2014. Dissolved organic matter quality and bioavailability changes across an urb nization gradient in headwater streams. Environ. Sci. Technol. 48, 7817−7824. https://doi.org/10.1021/es501422z

IPCC, 2013. In: T. F. Stocker, et al. (Eds.), Climate change 2013: The physical science basis. Contribution of Working Group I to the Fifth Assessment Report of the Intergovernmental Panel on Climate Change. Cambridge: Cambridge University Press. doi: 10.1017/CBO978110 324

Ivens, W.P., Tysmans, D.J., Kroeze, C., Löhr, A.J., van Wijnen, J., 2011. Modeling global N_2O emissions from aquatic systems. Curr. Opin. Environ. Sust. 3(5), 350−358. https://doi.org/10.1016/j.cosust.2011.07.007

Li, S.Y., Bush, R.T., Santos, I.R., Zhang, Q.F., Song, K.S., Mao, R., Wen, Z.D., Lu, X.X., 2018. Large greenhouse gases emissions from China's lakes and reservoirs. Water Res. 147, 13–24. https://doi.org/10.1016/j.watres.2018.09.053

Liang, X., Xing, T., Li, J.X., Wang, B.L., Wang, F.S., He, C.Q., Hou, L.J., Li, S.L., 2019. Control of the hydraulic load on nitrous oxide emissions from cascade reservoirs. Environ. Sci. Technol. 53(20), 11745−11754. https://doi.org/10.1021/acs.est.9b03438

Liu, J., Yang, S.Q., Jiang, C., 2013. Coastal reservoirs strategy for water resource development-a review of future trend. J. Water Resou. Prot. 5, 336−342. https://doi.org/10.4236/jwarp.2013.53A034

Liu, X.L., Liu, C.Q., Li, S.L., Wang, F.S., Wang, B.L., Wang, Z.L., 2011. Spatiotemporal variations of nitrous oxide (N_2O) emissions from two reservoirs in SW China. Atmos. Environ. 45 (31), 5458−5468. https://doi.org/10.1016/j.atmosenv.2011.06.074

Liu, X.L., Li, S.L., Wang, Z.L., Han, J.L., Li, J., Wang, B.L., Wang, F.S., Bai, L., 2017. Nitrous oxide (N_2O) emissions from a mesotrophic reservoir he Wujiang River, Southwest China. Acta Geochim. 36 (4), 667−679. https://doi.org/10.1007/s11631-017-0172-4

Maavara, T., Lauerwald, R., Laruelle, G.G. Akbarzadeh, Z., Bouskill, N.J., Van Cappellen, P., Regnier, P., 2019. Nitrous oxide emissio s from inland waters: Are IPCC estimates too high? Global Change Biol. 25, 473−488. https://doi.org/10.1111/gcb.14504

Monteiro, M., Séneca, J., Torgo, L., Cleary, D.F., Gomes, N.C., Santoro, A.E. and Magalhães, C., 2017. Environmental controls on estuarine nitrifying communities along a salinity gradient. Aquat. Microb. Ecol. 80(2), 167−180.

Musenze, R.S., Grinham, A., Werner, U., Gale, D., Sturm, K., Udy, J., Yuan, Z.G., 2014. Assessing the spatial and temporal variability of diffusive methane and nitrous oxide emissions from subtropical freshwater reservoirs. Environ. Sci. Technol. 48, 14499–14507. https://doi.org/10.1021/es505324h

Outram, F.N., Hiscock, K.M., 2012. Indirect nitrous oxide emissions from surface water bodies in a lowland arable catchment: a significant contribution to agricultural greenhouse gas budgets? Environ. Sci. Technol. 46, 8156–8163. https://doi.org/10.1021/es3012244

Phanwilai, S., Kangwannarakul, N., Noophan, P., Kasahara, T., Terada, A., Munakata-Marr, J., and Figueroa, L.A., 2020. Nitrogen removal efficiencies and microbial communities in full-scale

IFAS and MBBR municipal wastewater treatment plants at high COD:N ratio. Front. Environ. Sci. Eng. 14(6), 115. https://doi.org/10.1007/s11783-020-1374-2

Ravishankara, A.R., Daniel, J.S., Portmann, R.W., 2009. Nitrous oxide (N_2O): The dominant ozone-depleting substance emitted in the 21st century. Science 326, 123–125. https://doi.org/10.1126/science.1176985

Saikawa, E., Prinn, R.G., Dlugokencky, E., Ishijima, K., Dutton, G.S., Hall, B.D., Langenfelds, R., Tohjima, Y., Machida, T., Manizza, M., Rigby, M., O'Doherty, S., Patra, P.K., Harth, C.M., Weiss, R.F., Krummel, P.B., van der Schoot, M., Fraser, P.J., Steele, L.P., Aoki, S., Nakazawa,T., Elkins, J.W., 2014. Global and regional emissions estimates for $_2O$. Atmos. Chem. Phys. 14, 4617–4641. https://doi.org/10.5194/acp-14-4617-2014

Salk, K.R., Ostrom, P.H., Biddanda, B.A., Weinke, A Kendall, S.T., Ostrom, N.E., 2016. Ecosystem metabolism and greenhouse gas production in a mesotrophic northern temperate lake experiencing seasonal hypoxia. Biogeochemistry 131, 303−319. https://doi.org/10.1007/s10533-016-02

Sebilo, M., Billen, G., Mayer, B., Billiou, D., Grably, M., Garnier, J. and Mariotti, A., 2006. Assessing nitrification and denitrif tion in the Seine River and estuary using chemical and isotopic techniques. Ecosystems, 9(4), 564−577.

Shaaban, M., Wu, Y., Khalid, M. Peng, Q., Xu, X., Wu, L., Younas, A., Bashir, S., Mo, Y., Lin, S., Zafar-ul-Hye, M., A M., Hu, R., 2018. Reduction in soil N_2O emissions by pH manipulation and enhanced nosZ g ne transcription under different water regimes. Environ. Pollut. 235, 625–631. https://doi.org/10.1016/j.envpol.2017.12.066

Sitharam T.G., Yan S.Q., Falconer R., Sivakumar M., Jones B., Kolathayar S., Sinpoh L., 2020. Sustainable Water Resource Development Using Coastal Reservoirs. Elsevier, Cambridge, USA.

Sinha, E., Michalak, A.M., Balaji, V., 2017. Eutrophication will increase during the 21st century as a result of precipitation changes. Science 357, 405–408. https://doi.org/10.1126/science.aan2409

Stanley, E.H., Casson, N.J., Christel, S.T., Crawford, J.T., Loken, L.C., Oliver, S.K., 2016. The ecology of methane in streams and rivers: patterns, controls, and global significance. Ecol. Monogr. 86, 146–171. https://doi.org/10.1890/15-1027

Sun, Z.G., Wang, L.L., Tian, H.Q., Jiang, H.H., Mou, X.J., Sun, W.L., 2013. Fluxes of nitrous oxide and methane in different coastal Suaeda salsa marshes of the Yellow River estuary, China. Chemosphere 90, 856–865. https://doi.org/10.1016/j.chemosphere.2012.10.004

Taipale, S.J., Sonninen, E., 2009. The influence of preservation method and time on the $\delta^{13}C$ value of dissolved inorganic carbon in water samples. Rapid Commun. Mass Sp. 23(16), 2507-2510. https://doi.org/10.1002/rcm.4072

United Nations, 2018. SDG 6 Synthesis Report 2018 on Water and Sanitation, United Nations, New York.

Wang, X.F., He, Y.X., Yuan, X.Z., Chen, H., Peng, C ., Yue, J.S., Zhang, Q.Y., Diao, Y.B., Liu, S.S., 2017. Greenhouse gases concentrations and fluxes from subtropical small reservoirs in relation with watershed urbanization. Atmos. Environ. 154, 225–235. http://dx.doi.org/10.1016/j.atmosenv.2017.01.047

Wang, X.M., Hu, M.J., Ren, H.C., Li, J.B., Tong, C., Musenze, R.S., 2018. Seasonal variations of nitrous oxide fluxes and soil denitrification rates in subtropical freshwater and brackish tidal marshes of the Min River estuary. Sci. Total Environ. 616–617, 1404–1413. https://doi.org/10.10 citotenv.2017.10.175

Wanninkhof, R. 1992. Relationship between wind speed and gas exchange over the ocean. J. Geophys. Res. 97, 7373−7382. https://doi.org/10.1029/92jc00188

Weiss, R.F., Price, B.A., 1980. Nitrous oxide solubility in water and seawater. Mar. Chem. 8(4), 347–359. https://doi.org/10.1016/0304-4203(80)90024-9

Welti, N., Hayes, M., Lockington, D., 2017. Seasonal nitrous oxide and methane emissions across a subtropical estuarine salinity gradient. Biogeochemistry 132, 55–69. https://doi.org/10.1007/s10533-016-0287-4

Williams, C.J., Frost, P.C., Morales-Williams, A.M., Larson, J.H., Richardson, W.B., Chiandet, A.S., Xenopoulos, M.A., 2016. Human activities cause distinct dissolved organic matter composition across freshwater ecosystems. Glob. Change Biol. 22, 613-626. https://doi.org/10.1111/gcb.13094

World Meteorological Organization, 2019. WMO Greenhouse Gas Bulletin No. 15 (25 November 2019). https://library.wmo.int/doc_num.php?explnum_id=5455.pdf

Wu, S., Chen, J., Li, C., Kong, D., Yu, K., Liu, S.W., Zou, J.W., 2018. Diel and seasonal nitrous oxide fluxes determined by floating chamber and gas transfer equation methods in agricultural irrigation watersheds in southeast China. Environ. onit. Assess. 190, 122 https://doi.org/10.1007/s10661-018-6502-0

Xiao, Q.T., Xu, X.F., Zhang, M., Duan, H.T., Hu, Z.H., ng, W., Xiao, W., Lee, X.H., 2019a. Coregulation of nitrous oxide emissions by nitrogen and temperature in China' s third largest freshwater lake (Lake Taihu). Limnol. Oceanogr. 64, 1070–1086. https://doi.org/10.1002/lno.11098

Xiao, Q.T., Hu, Z.H., Fu, C.S., Bian, H., Lee, X.H., Chen, S.T., Shang, D.Y., 2019b. Surface nitrous oxide concentrations and fluxes fr water bodies of the agricultural watershed in Eastern China. Environ. Pollut. 251, 185–192. https://doi.org/10.1016/j.envpol.2019.04.076

Xiao, Q.T., Hu, Z.H., Hu, C.,, Towfiqul Islam A.R.M., Bian, H., Chen S.T., Liu, C., Lee, X.H., A highly agricultural r network in Jurong Reservoir watershed as significant CO_2 and CH_4 sources. Sci. Total Environ. 769, 144558. https://doi.org/10.1016/j.scitotenv.2020.144558

Yang, H., 2014. China must continue the momentum of green law. Nature 509, 535-535. https:doi.org/10.1038/509535a

Yang, H., Huang, X., Thompson, J.R., Flower, R.J., 2015. Enforcement key to China's environment. Science 347(6224), 834-835. https:doi.org/10.1126/science.347.6224.834-d

Yang, H., Flower, R.J., Thompson, J.R., 2013. Sustaining China's water resources. Science 339(6116), 141-141. https://doi.org/10.1126/science.339.6116.141-b

Yang, L.B., Yan, W.J., Ma, P., Wang, J.N., 2011. Seasonal and diurnal variations in N_2O concentrations and fluxes from three eutrophic rivers in Southeast China. J. Geogr. Sci. 21(5), 820–832. https://doi.org/10.1007/s11442-011-0882-1

Yang, S., Kelly, S., 2015. The use of coastal reservoirs and SPP strategy to provide sufficient high quality water to coastal communities. J. Geosci. Environ. Prot. 3(5), 80–92. https://doi.org/10.4236/gep.2015.35010

Yang, P., Yang, H., Sardans, J., Tong, C., Zhao, G.H., Peñuelas, J., Li, L., Zhang, Y.F., Tan, L.S., Chun, K. P., Lai, D.Y. F., 2020a. Large spatial variations in diffusive CH_4 fluxes from a subtropical coastal reservoir affected by sewage discharge in utheast China. Environ. Sci. Technol. 54, 14192-14203. https://dx.doi.org/10.1021/acs.est 03431

Yang, P., Yang, H., Lai, D.Y.F., Guo, Q.Q., Zhang, Y.F., , C., Xu, C.B., Li, X.F., 2020b. Large contribution of non-aquaculture period fluxes to the annual N_2O emissions from aquaculture ponds in Southeast China J. Hydrol. 582, 124550. https://doi.org/10.1016/j.jhydrol.2020.1 50

Yu, Z.J., Deng, H.G., Wang, D.Q., Ye, M.W., Tan, Y.J., Li, Y.J., Chen, Z.L., Xu, S.Y., 2013. Nitrous oxide emissions in the Shanghai riv network: implications for the effects of urban sewage and IPCC methodology. Global Change Biol. 19, 2999–3010. https://doi.org/10.1111/gcb.12290

Yu, Z.J., Wang, D.Q., Li, Y.J., Deng, H.G., Hu, B.B., Ye, M.W., Zhou, X.H., Da, L.J., Chen, Z.L., Xu, S.Y., 2017. Carb ioxide and methane dynamics in a human-dominated lowland coastal river network (Shanghai, China). J. Geophys. Res.-Biogeo. 122(7), 1738–1758. https://doi.org/10.1002/2017JG003798

Zhang, L., Wang, L., Yin, K.D., Lü, Y., Zhang, D.R., Yang, Y.Q., Huang, X.P., 2013. Pore water nutrient characteristics and the fluxes across the sediment in the Pearl River estuary and adjacent waters, China. Estuar. Coast. Shelf S.133, 182–192. https://doi.org/10.1016/j.ecss.2013.08.028

Zhao, Y., Wu, B.F., Zeng, Y., 2013. Spatial and temporal patterns of greenhouse gas emissions from Three Gorges Reservoir of China. Biogeosciences, 10(2), 1219–1230. https://doi.org/10.5194/bg–10–1219–2013

Zhou, S., He, Y., Yuan, X., Peng, S., Yue, J., 2017. Greenhouse gas emissions from different land-use areas in the littoral zone of the three gorges reservoir, china. Ecol. Eng. 100, 316–324. http://doi.org/10.1016/j.ecoleng.2017.01.003

Zhu, D., Chen, H., Yuan, X.Z., Wu, N., Gao, Y.H., Wu, Y., Zhang, Y.M., Peng, C.H., Zhu, Q.A., Yang, G., Wu, J.H., 2013. Nitrous oxide emissions from the surface of the Three Gorges Reservoir. Ecol. Eng. 60, 150–154. http://dx.doi.org/10.1016/j.ec eng.2013.07.049

Table 1. Summary of ANOVAs of the effects of sampling location, sampling time and their interactions on surface water N_2O concentration and emission in the Wenwusha Reservoir.

	Month	Reservoir basin*		Discharge type **				
		SB	NB	Section-I	Section-T	Section-R	Section-A	Section-N
N_2O concentration	**Nov 2018**	30.1±2.5	60.1±1.8	62.9±2.1**a**	67.6±4.5**a**	62.7±3.8**a**	47.5±3.1**b**	41.25±2.7**b**
(nmol L^{-1})	**May 2019**	19.7±1.9	64.3±2.3	79.9±4.1**ab**	59.61±9.2**b**	86.5±6.8**a**	43.9±3.6**bc**	35.62±3.2**c**
	Jun 2019	29.1±5.2	84.0±8.6	85.5±15.4**a**	43.97±11.9**b**	123.7±37.2**a**	63.1±13.2**b**	50.21±6.7**c**
	Average	26.3	69.5	76.1	57.1	91.0	51.5	42.4
N_2O emission	**Nov 2018**	53.5±6.5	158.2±13.2	326.8±36.6**a**	181.9±36.9**b**	213.3±55.4**b**	96.3±15.4**c**	83.77±8.2**c**
(μg m^{-2} h^{-1})	**May 2019**	30.3±5.8	118.9±6.7	116.9±7.5**ab**	96.9±20.7**bc**	165.4±16.3**a**	90.9±11.0**b**	60.57±7.8**c**
	Jun 2019	72.5±15.0	182.3±20.4	201.3±29.7**ab**	105.2±43.6**bc**	269.1±104.9**a**	127.1±27.4**b**	117.2±16.0**c**
	Average	52.1	153.1	215	128	215.9	104.8	87.2

*SB and NB represent the south basin (n = 22 sampling sites) and north basin (n = 64 sampling sites), respectively, and the values are significantly different between basins at the $p<0.05$ level for all surveys. **Different sections impacted by different discharge types: Section-I (industrial effluents; n = 4), Section-T (municipal sewage; n = 6), Section-R (river input; n = 7), Section-A (aquacultural effluent; n = 22) and Section-N (non-discharge; n = 64). Across each row, values that share at least one letter are not significantly different from each other ($p\geq0.05$) within the month. Average values are calculated across the three surveys for each column.

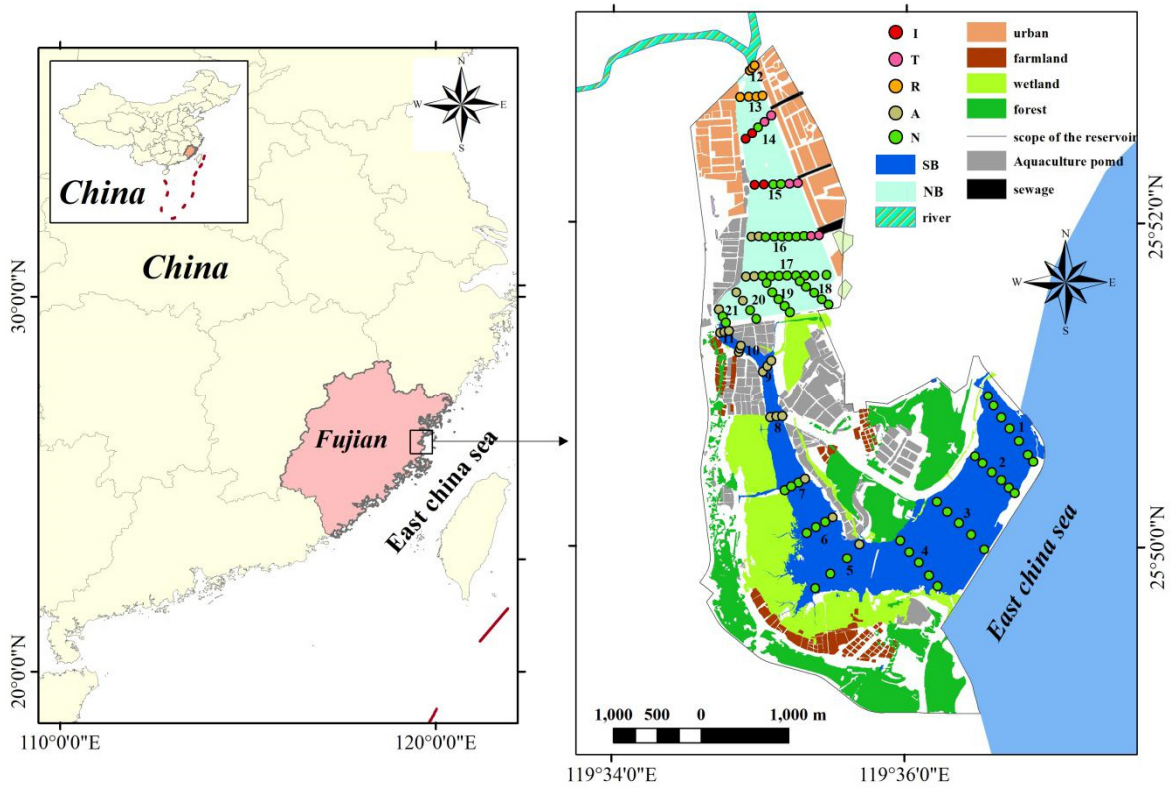

Fig. 1. Sampling sites within the Wenwusha Reservoir in Fujian Province, southeastern China. A total of 21 transects were sampled, with 11 transects in the south basin (SB) (1–11), and 10 in the north basin (NB) (12–21). Each circle represents a sampling site influenced by different discharge type: A: aquacultural effluent (n = 4); I: industrial effluent (n = 6); R: river input (n = 7); T: municipal sewage (n = 22); N: non-discharge (n = 64).

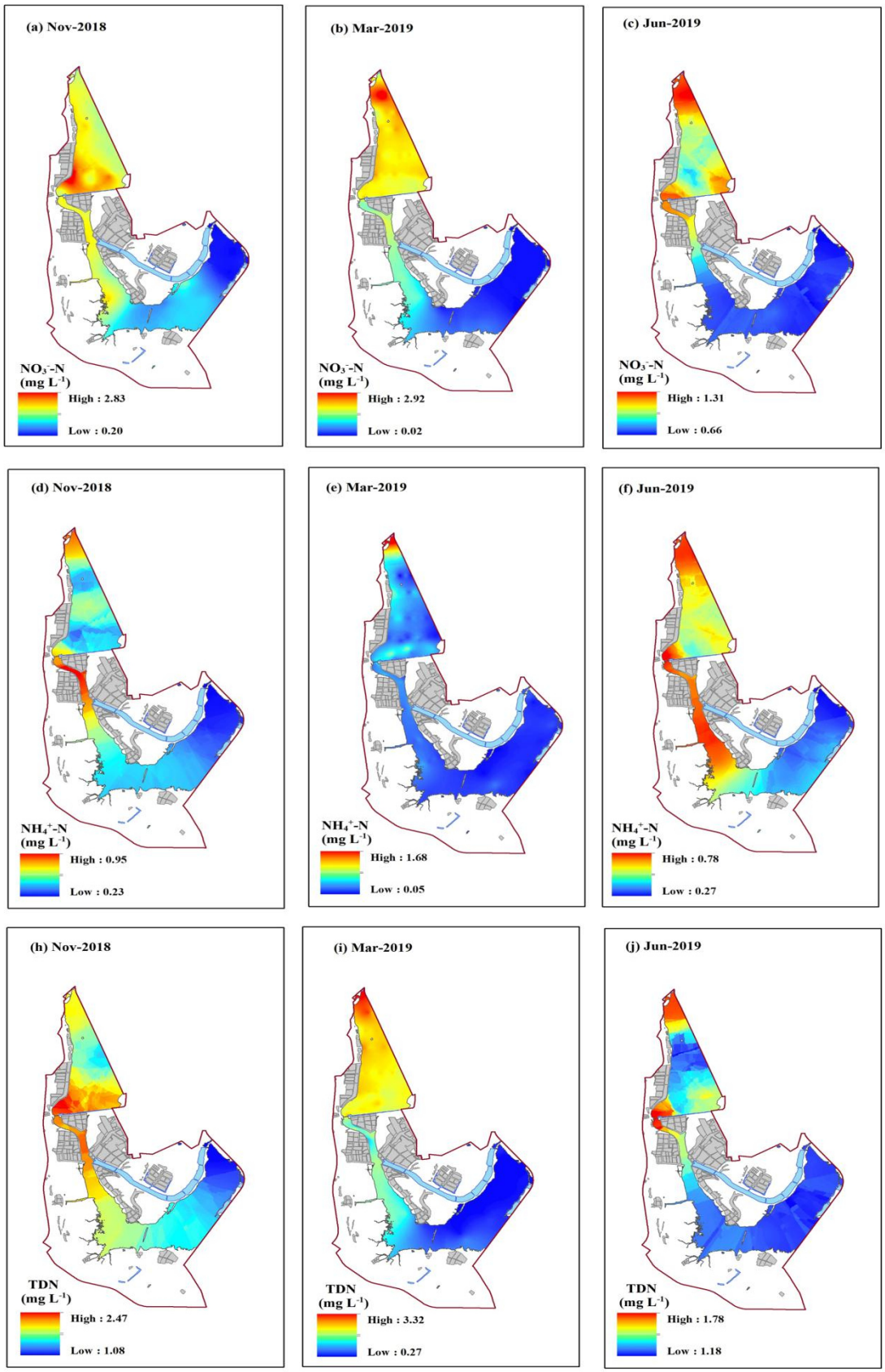

Fig. 2. Spatial distributions of surface-water NO_3^--N (*a-c*), NH_4^+-N (*d-f*) and TDN (*g-i*) in the Wenwusha Reservoir.

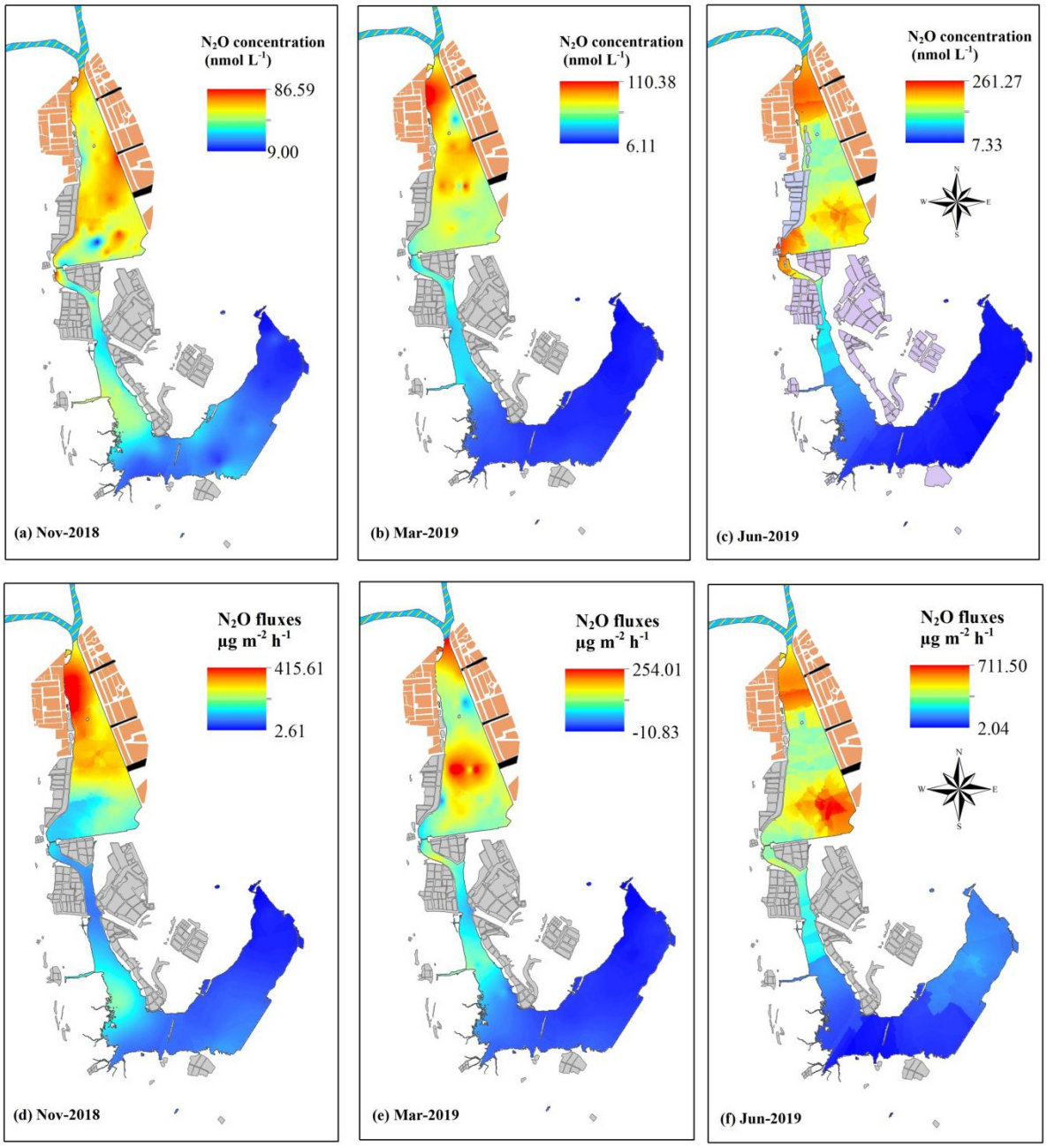

Fig. 3. Spatial distributions of surface-water N_2O concentration (*a-c*) and fluxes (*d-f*) in the Wenwusha Reservoir.

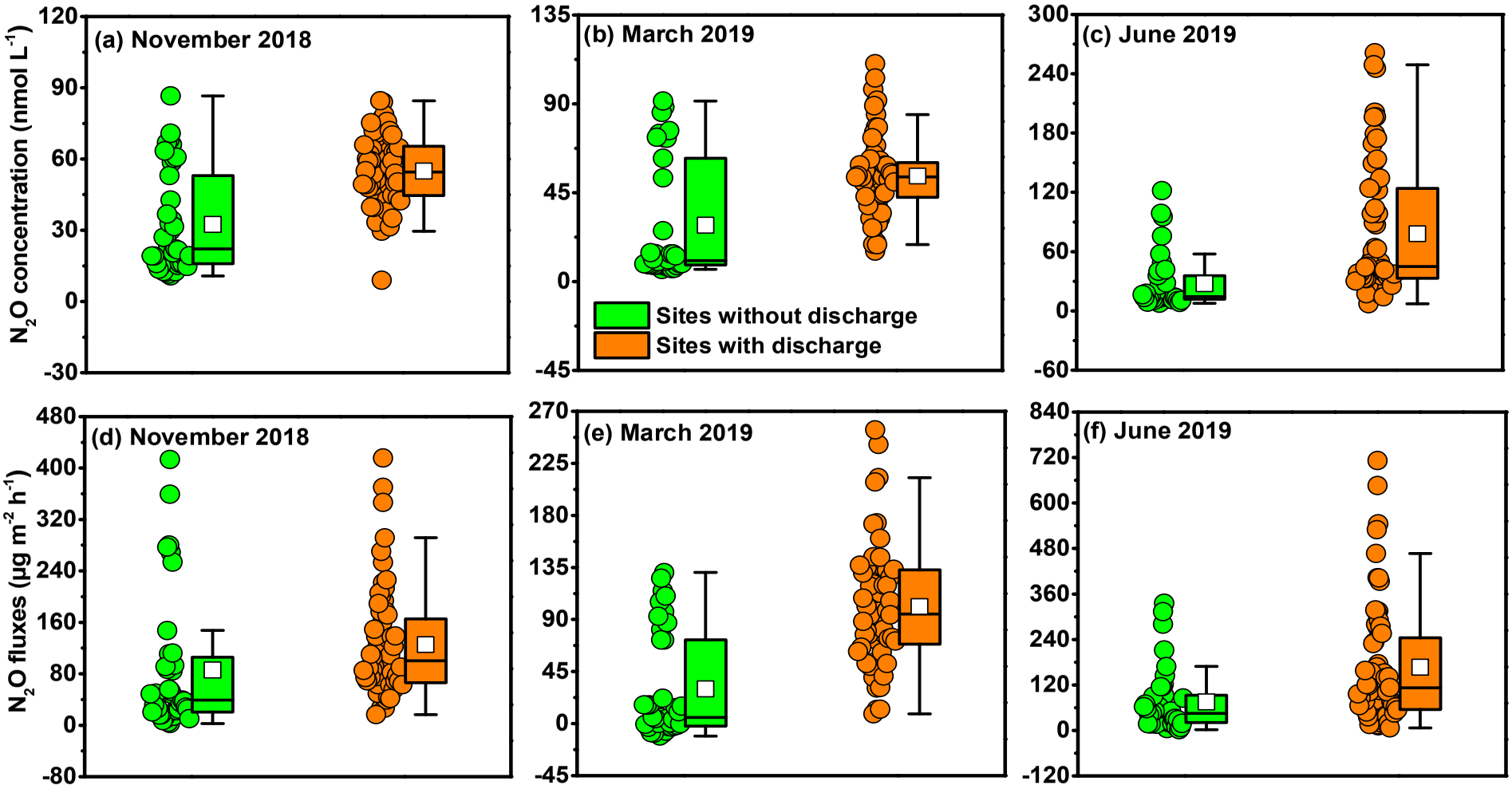

Fig. 4. Boxplots of dissolved N_2O concentrations and N_2O fluxes for sampling sites with or without discharge. Each box shows the quartiles and median, while the square and whiskers represent the mean and values within 1.5 times of the interquartile range, respectively. Sites with discharge (n = 64) and without discharge (n = 39) are significantly different from each other (p<0.05) in all cases.

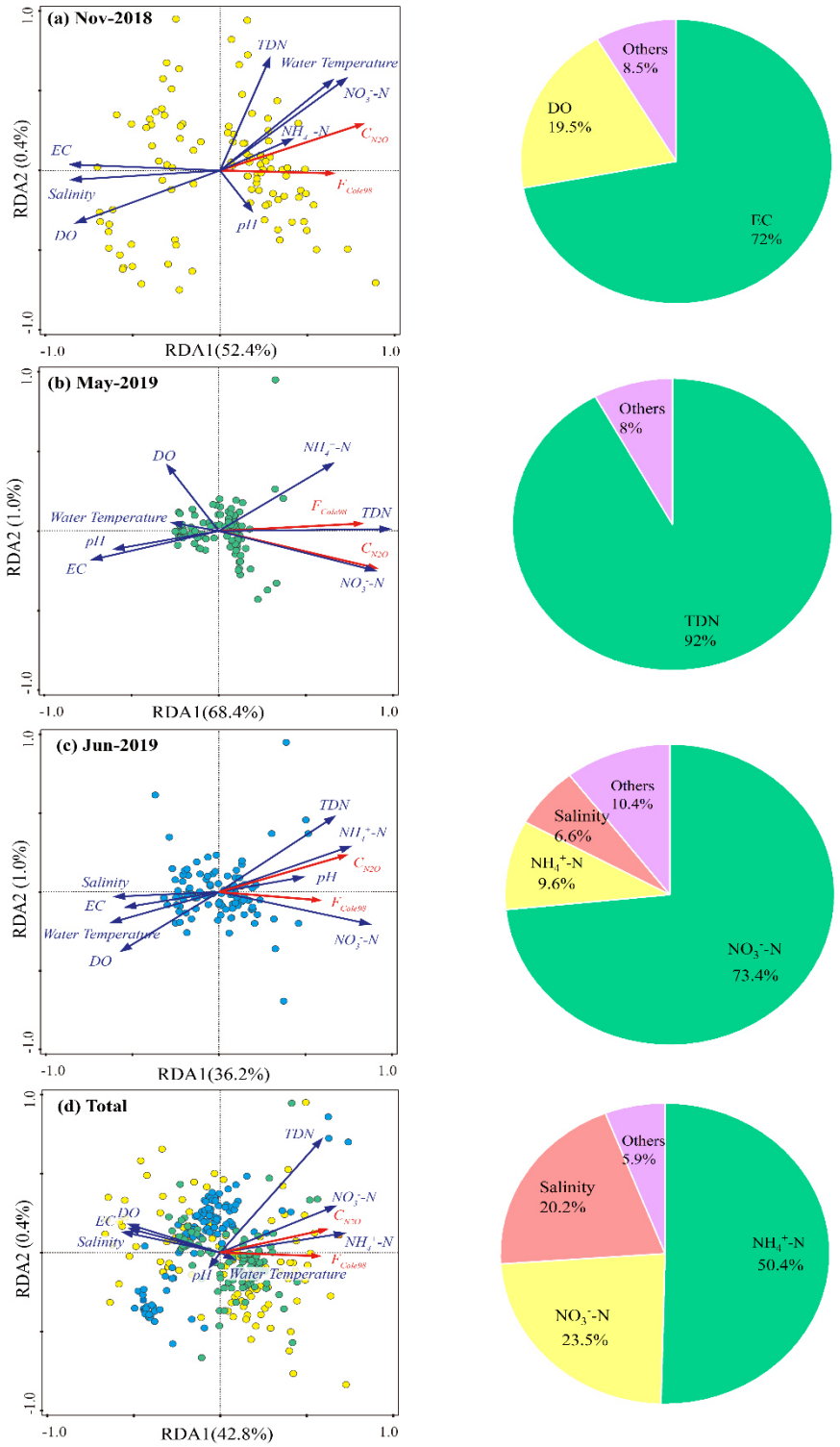

Fig. 5. The redundancy analysis (RDA) biplots of the N_2O concentration / emission and hydrographical parameters in the Wenwusha Reservoir. The loadings of ancillary hydrographical parameters (arrows) and the scores of observations in the survey of November 2018 (*a*), March 2019 (*b*) and June 2019 (*c*) and combined data from all surveys (*d*). W_T, *EC, DO,* C_{N2O} and F_{Cole98} represent water temperature, conductivity, dissolved oxygen, dissolved N_2O concentration and N_2O emission, respectively. The pie charts show the percentages of variance explained by the different parameters.

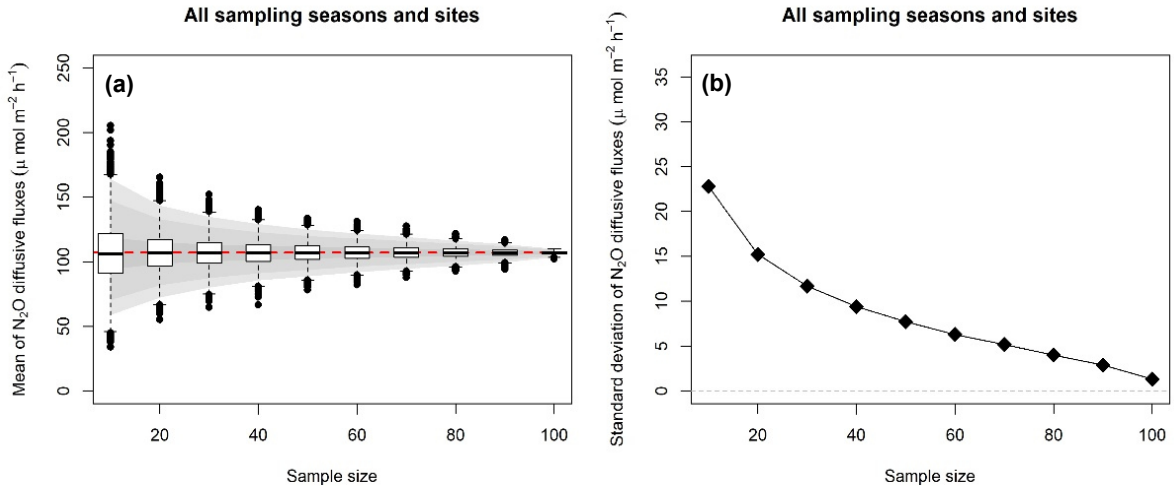

Fig. 6. (a) The box and whisker plots and (b) standard deviation of estimated N_2O fluxes from the Wenwusha Reservoir. Monte Carlo analysis was used to evaluate the effect of sample size on the emission estimate. Without replacements, the N_2O emission measurements were resampled from all sites (n = 10, 20, 30…, 100). The resampling process was repeated 10,000 times. For each sample size, the overall mean and standard deviation of N_2O emission were calculated. The N_2O emission are a function of the number of sampling sites selected from a total of 103 sites based on 1000 simulations. In panel *a*, the margins of the boxes are the upper and lower quartiles, and the line in the box represents the median. The whiskers are the extreme values that fall within 1.5 times the interquartile range and the circles represent extreme values that fall outside 1.5 times the interquartile range. The red line are the overall average N_2O flux based on the results from all 103 sites. The grey areas represent 70, 95 and 99% of the Highest Probability Density ranges.

Supporting Information

Coastal reservoirs as a source of the greenhouse gas nitrous oxide: spatial-temporal patterns and assessment strategy

Ping Yang[a,b], Miaohui Lu[a,b], Kam W. Tang[c], Hong Yang[d,e,f], Derrick Y. F. Lai[g], Chuan Tong[a,b*], Kwok Pan Chun[h], Linhai Zhang[a,b], Chen Tang[b]

[a]*Key Laboratory of Humid Subtropical Eco-geographical Process of Ministry of Education, Fujian Normal University, Fuzhou 350007, P.R. China*

[b]*School of Geographical Sciences, Fujian Normal University, Fuzhou 350007, P.R. China*

[c]*Department of Biosciences, Swansea University, Swansea SA2 8PP, U. K.*

[d]*College of Environmental Science and Engineering, Fujian Normal University, Fuzhou 350007, P.R. China*

[e]*Collaborative Innovation Center of Atmospheric Environment and Equipment Technology, Jiangsu Key Laboratory of Atmospheric Environment Monitoring and Pollution Control (AEMPC), School of Environmental Science and Engineering, Nanjing University of Information Science & Technology, 219 Ningliu Road, Nanjing 210044, China*

[f]*Department of Geography and Environmental Science, University of Reading, Reading, RG6 6AB, UK*

[g]*Department of Geography and Resource Management, The Chinese University of Hong Kong, Hong Kong, China*

[h]*Department of Geography, Hong Kong Baptist University, Hong Kong, China*

***Correspondence to:**

tongch@fjnu.edu.cn (Chuan Tong)

Supporting Information Summary

No. of pages: 13 No. of figures: 4 No. of tables: 4

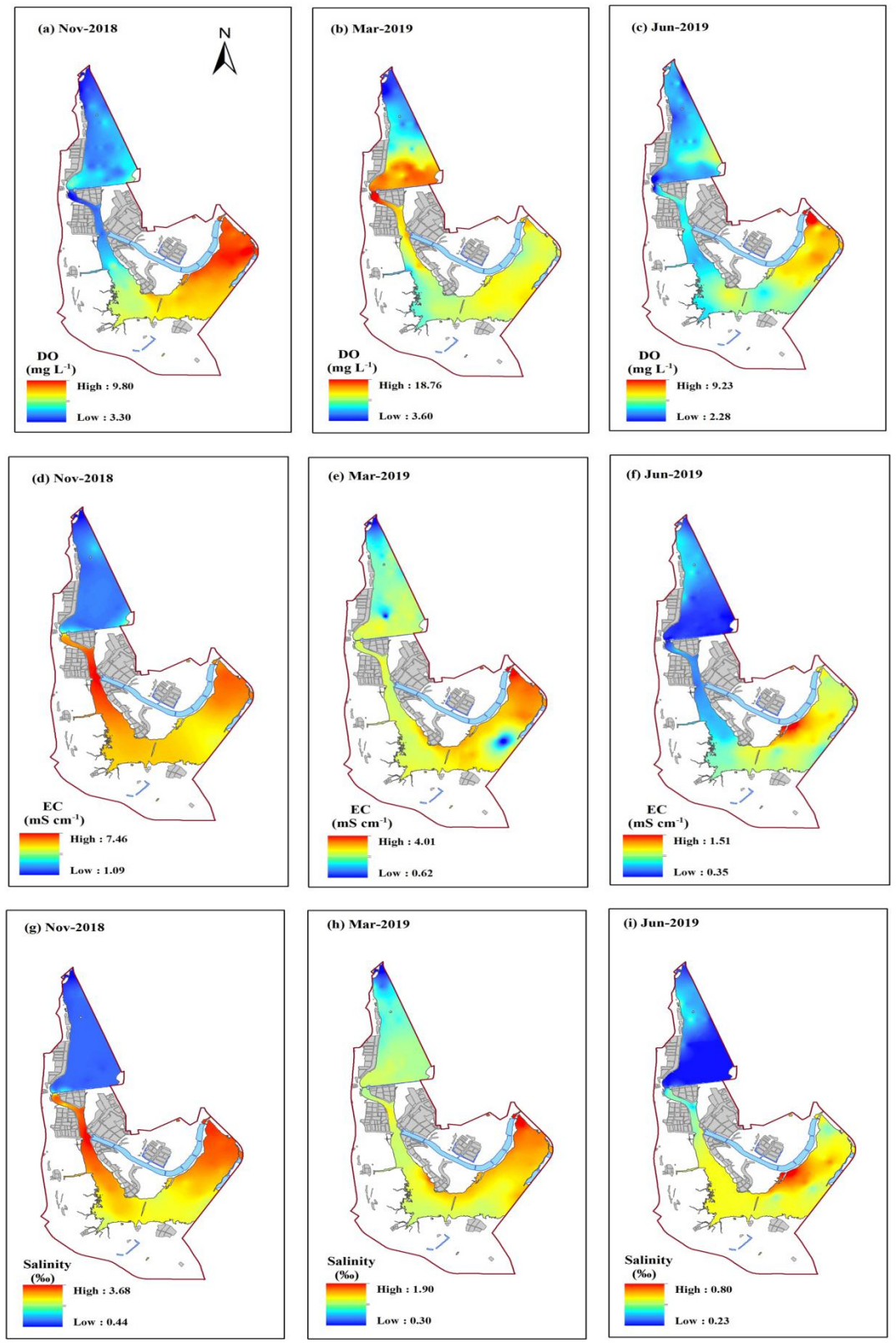

Fig. S1. Spatial distributions of surface-water DO (*a–c*), electrical conductivity (EC) (*d-f*), and salinity (*g–i*) in the Wenwusha Reservoir.

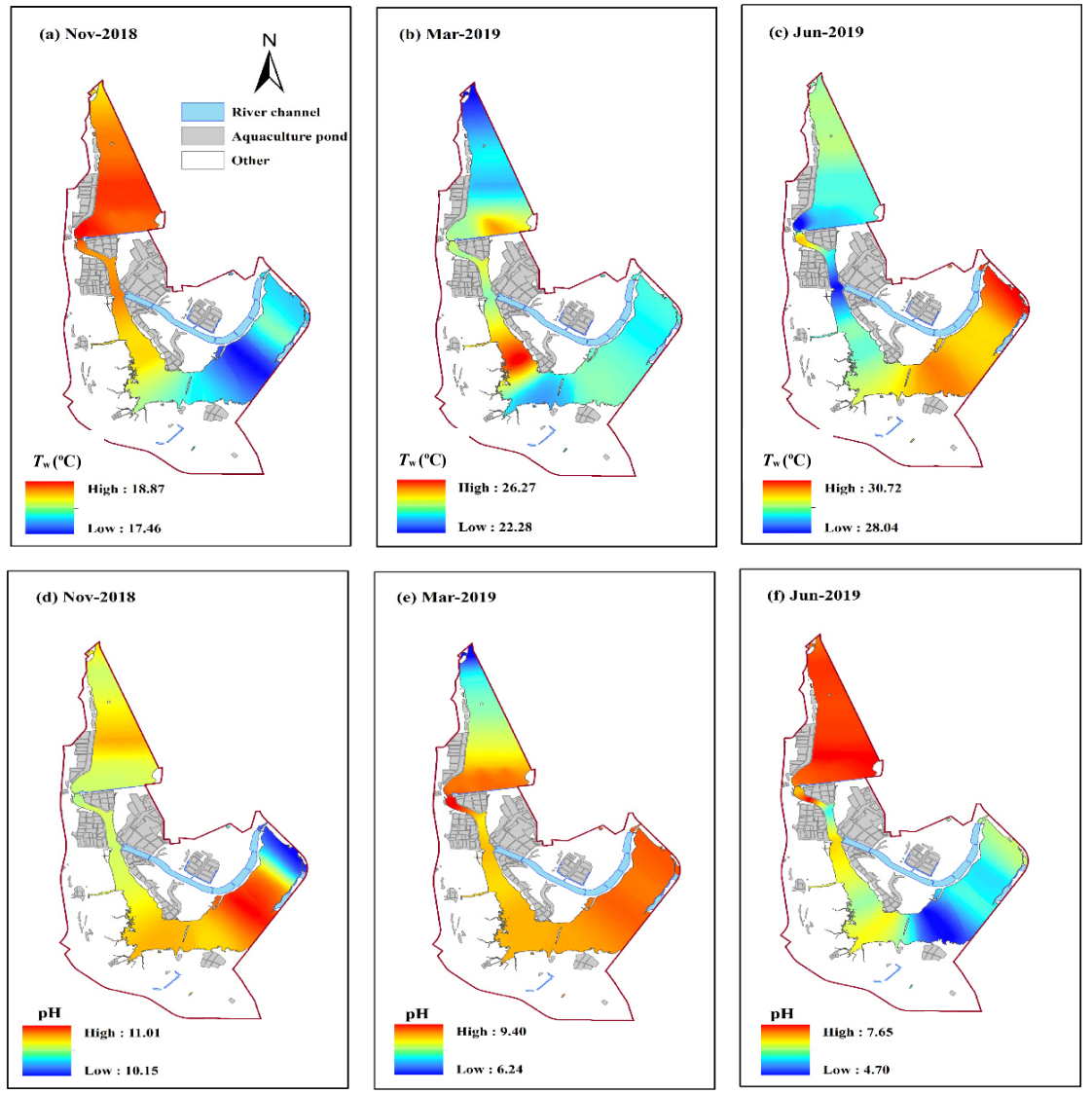

Fig. S2. Spatial distributions of surface-water T_W (a-*c*), and pH (*d–f*) in the Wenwusha Reservoir.

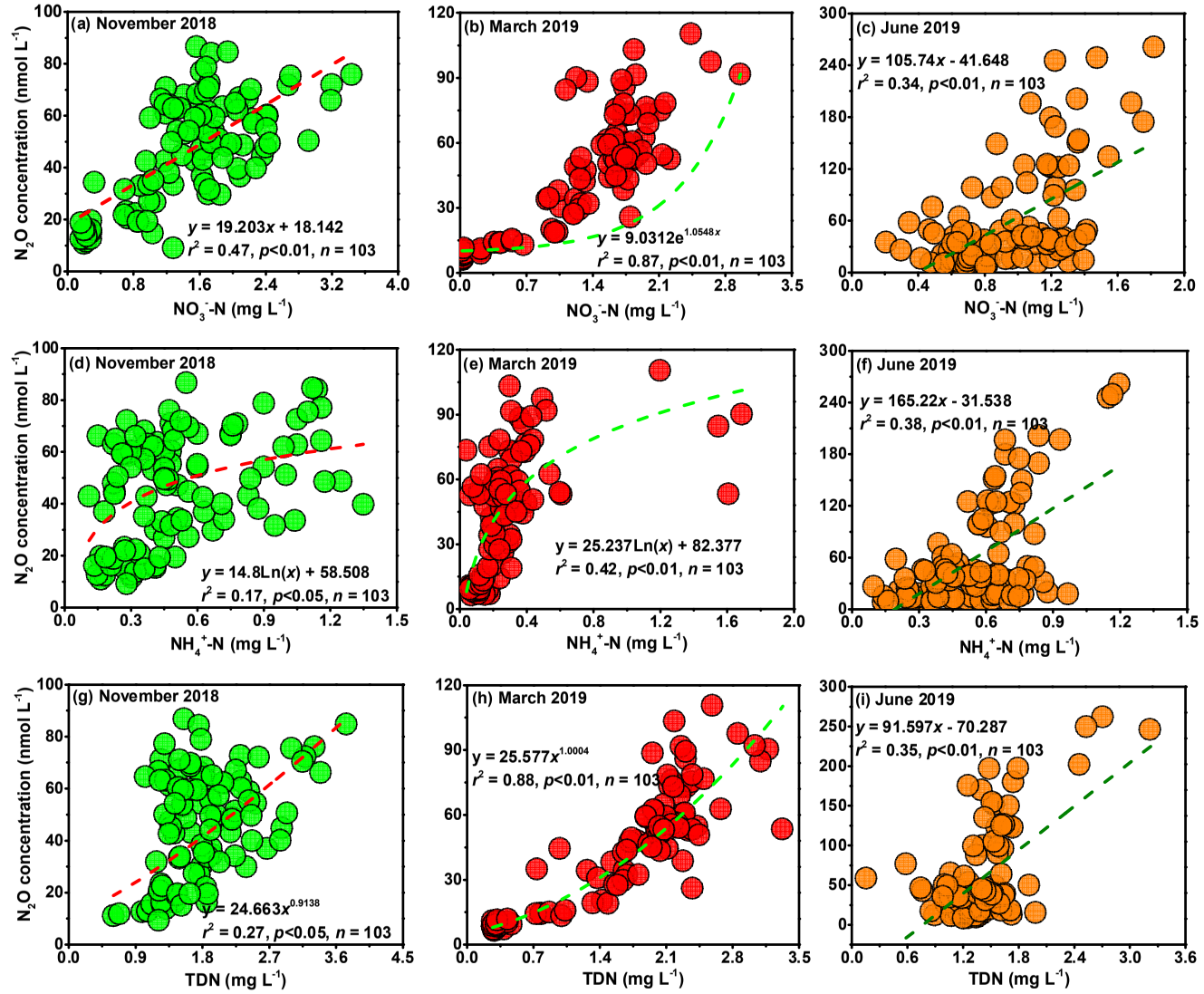

Fig. S3. Relationships between surface-water N_2O concentration and NO_3^--N, NH_4^+-N and TDN concentrations in the Wenwusha Reservoir. Parameter bounds on the regression coefficients are at 95% confidence limits.

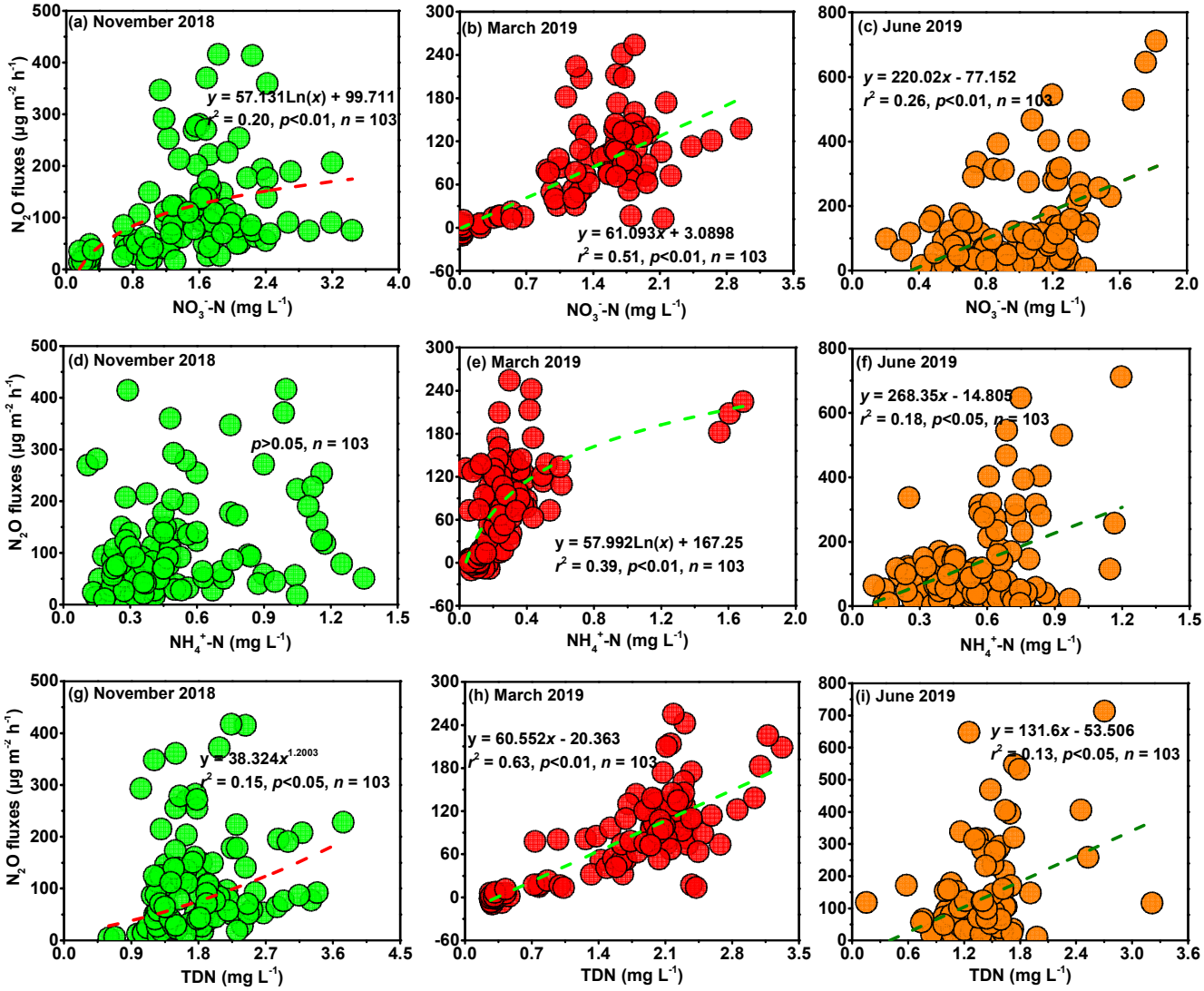

Fig. S4. Relationships between N_2O fluxes and surface-water NO_3^--N, NH_4^+-N and TDN concentrations in the Wenwusha Reservoir. Parameter bounds on the regression coefficients are at 95% confidence limits.

Table S1. Hydrographical parameters in the different areas based on discharge types in the Wenwusha Reservoir.

Month	Discharge Area#	DO (mg L^{-1})*	Salinity (‰)*	NO_3^--N (mg L^{-1})	NH_4^+-N (mg L^{-1})*	TDN (mg L^{-1})
Nov-2018	**Section-I**	4.50±0.28**ab**	1.08±0.02**a**	1.96±0.22**a**	0.53±0.16**c**	1.87±0.20**a**
	Section-T	4.89±0.17**ab**	1.10±0.00**a**	1.55±0.08**ab**	0.53±0.03**c**	1.60±0.08**b**
	Section-R	3.50±0.30**a**	0.82±0.13**a**	1.59±0.09**ab**	1.28±0.16**a**	2.00±0.14**ab**
	Section-A	4.76±0.19**b**	2.44±0.21**b**	1.91±0.12**a**	0.72±0.06**b**	2.23±0.12**a**
	Section-N	6.52±0.21**c**	2.01±0.12**b**	1.27±0.10**b**	0.41±0.03**d**	1.67±0.07**b**
	Average	4.83	1.49	1.66	0.69	1.87
Mar-2019	**Section-I**	8.69±0.21**b**	1.08±0.02**b**	1.69±0.12**a**	0.41±0.05**b**	2.31±0.15**ab**
	Section-T	8.61±1.01**b**	1.15±0.02**b**	1.84±0.08**a**	0.40±0.08**b**	2.18±0.07**ab**
	Section-R	4.32±0.61**a**	0.66±0.13**a**	1.98±0.29**a**	0.97±0.23**a**	2.93±0.13**a**
	Section-A	9.71±0.69**c**	1.27±0.02**b**	1.40±0.08**a**	0.50±0.04**b**	1.75±0.09**b**
	Section-N	13.04±0.31**d**	1.37±0.03**c**	1.01±0.10**b**	0.20±0.01**c**	1.36±0.11**c**
	Average	8.87	1.11	1.58	0.50	2.11
Jun-2019	**Section-I**	4.02±0.23**a**	0.45±0.03**a**	1.14±0.23**ab**	0.59±0.13**bc**	1.24±0.38**bc**
	Section-T	4.75±0.32**ab**	0.35±0.02**a**	1.08±0.16**b**	0.48±0.07**c**	1.22±0.11**bc**
	Section-R	4.18±0.66**a**	0.36±0.03**a**	1.35±0.12**a**	0.96±015**a**	2.06±0.18**a**

	Section-A	4.44±0.20**a**	0.45±0.02**a**	0.99±0.06**b**	0.68±0.05**b**	1.56±0.11**b**
	Section-N	5.62±0.16**b**	0.46±0.02**a**	0.90±0.04**b**	0.50±0.03**c**	1.08±0.04**c**
	Average	4.60	0.41	1.09	0.64	1.43

[#]Different sections impacted by different discharge types: Section-I (industrial effluents; $n = 4$), Section-T (municipal sewage; $n = 6$), Section-R (river input; $n = 7$), Section-A (aquacultural effluent; $n = 22$) and Section-N (non-discharge; $n = 64$). DO, and TDN represent dissolved oxygen and total dissolved nitrogen, respectively. Different letters across each row indicate significant differences at the $p<0.05$ level. Averages across sections are calculated for each month. *Data are taken from Yang et al. (2020).

Table S2. Pearson correlation coefficients between N_2O concentration / emission and different environmental variables in the Wenwusha Reservoir.

Environmental variables	N_2O concentration				N_2O emission			
	Nov-2018	Mar-2019	Jun-2019	All data	Nov-2018	Mar-2019	Jun-2019	All data
Meteorologic variables								
Air temperature	0.602**	NS	NS	0.224*	0.373**	NS	NS	0.193**
Wind speed	NS	-0.607**	NS	-0.265*	NS	-0.300**	NS	-0.127*
Atmospheric pressure	NS	NS	NS	NS	NS	NS	NS	NS
Hydrographical parameters								
Water temperature	0.754**	NS	-0.495**	NS	0.453**	NS	-0.346**	NS
pH	NS	-0.508**	0.374**	NS	NS	-0.490**	0.274**	NS
Conductivity (EC)	-0.682**	-0.607**	-0.412**	-0.296**	-0.548**	-0.597**	-0.303**	-0.299**
Salinity	-0.705**	-0.738**	-0.442**	-0.322**	-0.543**	-0.715**	-0.343**	-0.320**
Dissolved oxygen (DO)	-0.763**	-0.358**	-0.495**	-0.294**	-0.522**	-0.219*	-0.304**	-0.302**
NO_3^--N	0.687**	0.859**	0.586**	0.445**	0.403**	0.716**	0.511**	0.369**
NH_4^+-N	0.391*	0.487**	0.619**	0.452**	0.260**	0.551**	0.422**	0.402**
TDN	0.434**	0.873**	0.596**	0.460**	NS	0.796**	0.359**	0.316**

The symbols * and ** denote significant correlations at $p < 0.05$ and $p < 0.01$, respectively. NS means non-significant relationship.

Table S3. Comparison of the N_2O fluxes (μg m^{-2} h^{-1}) in reservoirs and lakes across different countries and climate zones.

Ecosystem Type	Location	Climate	N_2O emission	Reference
Reservoirs	Samuel Reservoir and Tucurui Reservoir, Brazil	Tropical	229.2	Lima et al., 2002
	Petit Saut Reservoir and Fortuna Reservoir	Tropical	−247.5 to 401.6 (167.2)	Guérin et al., 2008
	Serra de Mesa Reservoir, Brazil	Tropical	5.7	Sikar et al., 2005
	Manso Reservoir, Brazil	Tropical	5.7	Sikar et al., 2005
	Three Gorges Reservoir, China	Subtropical	-0.64 to 5.17 (---)	Yu et al., 2018
	Chongqing, Southwest China	Subtropical	3.67 to 1221.0 (240.17)	Wang et al., 2017a
	Hongjiadu Reservoir, China	Subtropical	4.4 to 58.1 (19.8)	Liu et al., 2011a
	Wujiangdu Reservoir, China	Subtropical	3.5 to 77.4 (28.2)	Liu et al., 2011a
	Dongfeng Reservoir, China	Subtropical	0.4 to 26.8 (8.4)	Liu et al., 2017
	Jinghong Reservoir, China	Subtropical	0.6 to 1.1 (---)	Shi et al., 2020
	Southeast Queensland, Australia	Subtropical	−0.2 to 3.5 (0.4)	Musenze et al., 2014
	Wenwusha Reservoir, China	Subtropical	−10.8 to 711.5 (107.0)	**This study**
	Xiaolangdi Reservoir, China	Temperate	24.2 to 25.1 (24.8)	Cheng et al., 2019
	Eguzon Reservoir, France	Temperate	4.9 to 142.1 (31.5)	Descloux et al., 2017
	Lokka Reservoir, Finland	Temperate	-3.5 to 11.4 (---)	Huttunen et al., 2002
	Porttipahta Reservoir, Finland	Temperate	-0.9 to 10.6 (---)	Huttunen et al., 2002

Lakes	Taihu Lake, China	Subtropical	18.04 to 25.5 (---)	Wang et al., 2009
	Poyang Lake, China	Subtropical	−9.73 to 127.0 (---)	Wang et al., 2017b
	Lake Nakaumi, Japan	Subtropical	31.2 to 78.8 (47.1)	Hirota et al., 2007
	Lake Yuqiao and 6 other lakes, Tianjin, China	Temperate	−6.2 to 39.2 (7.9)	Liu et al., 2015
	Lake Kevätön, Finland	Temperate	3.96 to 22.00	Huttunen et al., 2003
	Lake Mochou, Antarctica	Polar climate	−8.2 to 68.5 (9.7)	Liu et al., 2011b
	Lake Tuanjie, Antarctica	Polar climate	−11.8 to 18.0 (7.9)	Liu et al., 2011b
	Lake Daming, Antarctica	Polar climate	−35.6 to 45.2 (22.4)	Liu et al., 2011b
	Lakes on the Tibetan Plateau, China	Plateau-climate	0.1 to 38.3 (11.9)	Yan et al., 2018

Numbers in brackets are averages. “---” indicates no data.

References

Cheng, F., Zhang, H.M., Zhang, G.L., Liu, S.M., Song, G.D., Du, G.X., 2019. Distribution and emission of N_2O in the largest river-reservoir system along the Yellow River. Sci. Total Environ. 666, 1209–1219. https://doi.org/10.1016/j.scitotenv.2019.02.277

Descloux, S., Chanudet, V., Serça, D., Guérin, F., 2017. Methane and nitrous oxide annual emissions from an old eutrophic temperate reservoir. Sci. Total Environ. 598, 959–972. https://doi.org/10.1016/j.scitotenv.2017.04.066

Hirota, M., Senga, Y., Seike, Y., Nohara, S., Kunii, H., 2007b. Fluxes of carbon dioxide, methane and nitrous oxide in two contrastive fringing zones of coastal lagoon, Lake Nakaumi, Japan. Chemosphere 68 (3), 597−603. https://doi.org/10.1016/j.chemosphere.2007.01.002

Huttunen, J.T., Alm, J., Liikanen, A., Juutinen, S., Larmola, T., Hammar, T., Silvola, J., Martikainen, P.J., 2003. Fluxes of methane, carbon dioxide and nitrous oxide in boreal lakes and potential anthropogenic effects on the aquatic greenhouse gas emissions. Chemosphere 52, 609−621. https://doi.org/10.1016/S0045-6535(03)00243-1

Huttunen, J.T., Vaisanen, T.S., Hellsten, S.K., Heikkinen, M., Nykanen, H., Jungner, H., Niskanen, A., Virtanen, M.O., Lindqvist, O.V., Nenonen, O.S., Martikainen, P.J., 2002. Fluxes of CH_4, CO_2, and N_2O in hydroelectric reservoirs Lokka and Porttipahta in the northern boreal zone in Finland. Glob Biogeochem Cy. 16(1), 1003. https://doi.org/10.1029/2000GB001316

Guérin, F., Abril, G., Tremblay, A., Delmas, R., 2008. Nitrous oxide emissions from tropical hydroelectric reservoirs. Geophys. Res. Lett. 35(6), L06404. https://doi.org/10.1029/2007GL033057

Lima, I.B.T., Victoria, R.L., Novo, E.M.L.M., Feigl, B.J., Ballester, M.V.R., Ometto, J.P., 2002. Methane, carbon dioxide and nitrous oxide emissions from two Amazonian reservoirs during high water table. Verh. Internat. Verein. Limnol. 28, 438-442. https://doi.org/10.1080/03680770.2001.11902620

Liu, X.L., Li, S.L., Wang, Z.L., Han, G.L., Li, J., Wang, B.L., Wang, F.S., Bai, L., 2017. Nitrous oxide (N_2O) emissions from a mesotrophic reservoir on the Wujiang River, southwest China.

93 Acta Geochim 36(4), 667-679. https://doi.org/10.1007/s11631-017-0172-4

94 Liu, X.L., Liu, C.Q., Li, S.L., Wang, F.S., Wang, B.L., Wang, Z.L., 2011a. Spatiotemporal variations
95 of nitrous oxide (N_2O) emissions from two reservoirs in SW China. Atmos. Environ. 45 (31),
96 5458-5468. https://doi.org/10.1016/j.atmosenv.2011.06.074.

97 Liu, X.L., Bai, L., Wang, Z.L., Li, J., Yue, F.J., Li, S.L., 2015. Nitrous oxide emissions from river
98 network with variable nitrogen loading in Tianjin, China. J. Geochem. Explor. 157, 153-161.
99 https://doi.org/10.1016/j.gexplo.2015.06.009.

100 Liu, Y.S., Zhu, R.B., Ma, D.W., Xu, H., Luo, Y.H., Huang, T., Sun, L.G., 2011b. Temporal and
101 spatial variations of nitrous oxide fluxes from the littoral zones of three alga-rich lakes in coastal
102 Antarctica. Atmos. Environ. 45, 1464–1475. https://doi.org/10.1016/j.atmosenv.2010.12.017

103 Musenze, R.S., Grinham, A., Werner, U., Gale, D., Sturm, K., Udy, J., Yuan, Z.G., 2014. Assessing
104 the spatial and temporal variability of diffusive methane and nitrous oxide emissions from
105 subtropical freshwater reservoirs. Environ. Sci. Technol. 48, 14499–14507.
106 https://doi.org/10.1021/es505324h

107 Shi, W.Q., Chen, Q.W., Zhang, J.Y., Liu, D.S., Yi, Q.T., Chen, Y.C., Ma, H.H., Hu, L.M., 2020.
108 Nitrous oxide emissions from cascade hydropower reservoirs in the upper Mekong River.
109 Water Res. 2020, 115582. https://doi.org/10.1016/j.watres.2020.115582

110 Sikar, E., Santos, M.A., Matvienko, B., Silva, M.B., Rocha, C.H.E.D., Santos, E., Bentes, A.P.B.,
111 Rosa, L., 2005. Greenhouse gases and initial findings on the carbon circulation in two
112 reservoirs and their watersheds. Verh. Internat. Verein. Limnol. 29, 573-576.
113 https://doi.org/10.1080/03680770.2005.11902741

114 Wang, X.F., He, Y.X., Yuan, X.Z., Chen, H., Peng, C.H., Yue, J.S., Zhang, Q.Y., Diao, Y.B., Liu,
115 S.S., 2017a. Greenhouse gases conce ntration s and fluxes from subtropical small reservoirs in
116 relation with watershed urbanization. Atmos. Environ. 154, 225–235.
117 http://dx.doi.org/10.1016/j.atmosenv.2017.01.047

Wang, H.X., Zhang, L., Yao, X..L., Xue, B., Yan, W.J., 2017b. Dissolved nitrous oxide and emission relating to denitrification across the Poyang Lake aquatic continuum. J. Environ. Sci. 52, 130-140. http://dx.doi.org/10.1016/j.jes.2016.03.021

Yan, F., Sillanpää, M., Kang, S., Aho, K.S., Qu, B., Wei, D., Li, X.F., Li, C.L., Raymond, P.A., 2018. Lakes on the Tibetan Plateau as conduits of greenhouse gases to the atmosphere. J. Geop hys. Res.-Biogeo. 123, 2091–2103. https://doi.org/10.1029/2017JG004379

Yang, P., Yang, H., Sardans, J., Tong, C., Zhao, G.H., Peñuelas, J., Li, L., Zhang, Y.F., Tan, L.S., Chun, K. P., Lai, D.Y. F., 2020. Large spatial variations in diffusive CH_4 fluxes from a subtropical coastal reservoir affected by sewage discharge in southeast China. Environ. Sci. Technol. 54, 14192-14203. https://dx.doi.org/10.1021/acs.est.0c03431

Yu, J.H., Zhang, J.Y., Chen, Q.W., Yu, W.Y., Hu, L.M., Shi, W.Q., Zhong, J.C., Yan, W.X., 2018. Dramatic source-sink transition of N2O in the water level fluctuation zone of the Three Gorges Reservoir during flooding-drying processes. Environ. Sci. Pollut. Res. 25, 20023-20031. https://doi.org/10.1007/s11356-018-2190-0.